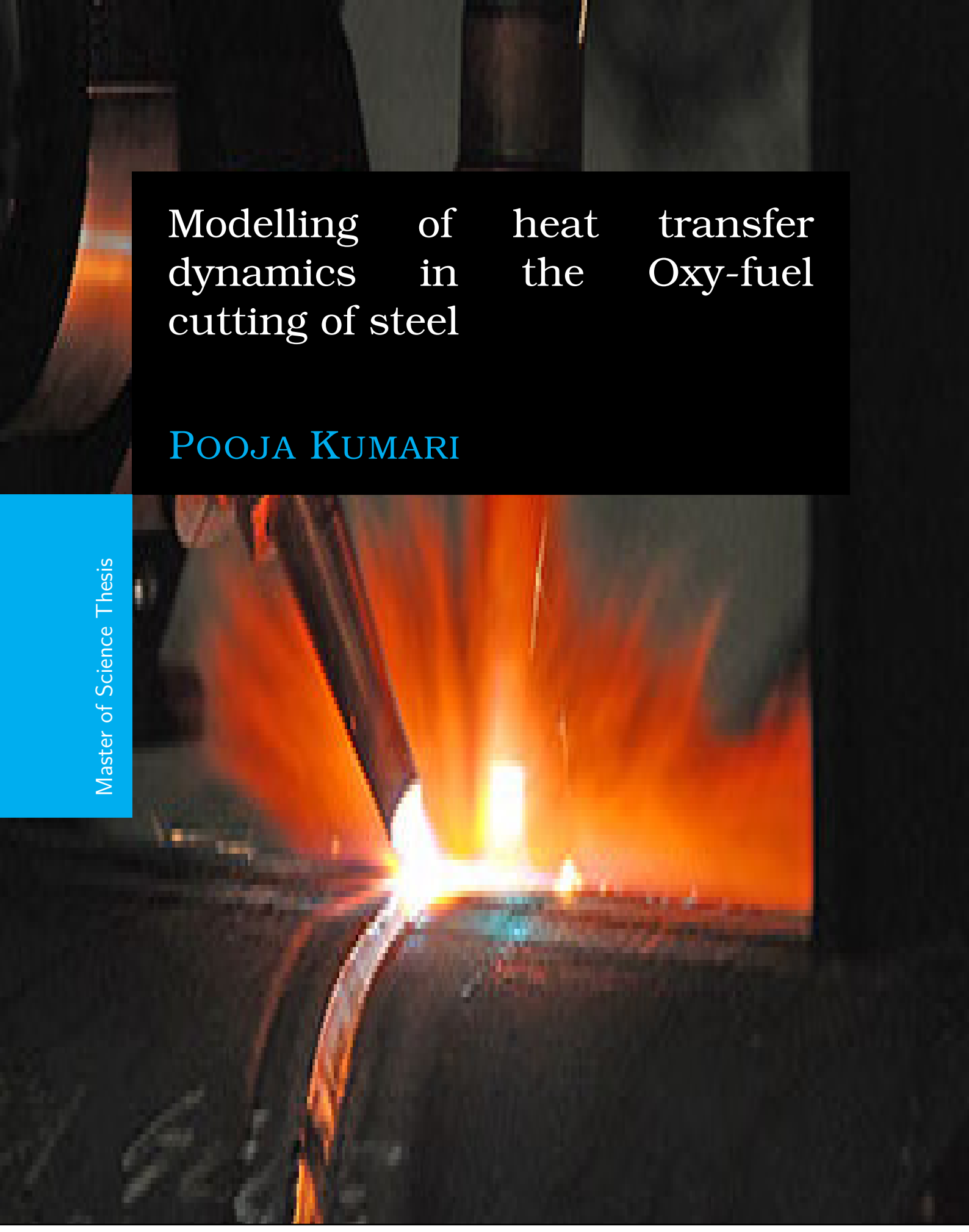

Modelling of heat transfer dynamics in the Oxy-fuel cutting of steel

Pooja Kumari

Master of Science Thesis

TU Delft Delft University of Technology

Delft Center for Systems and Control

Modelling of heat transfer dynamics in the Oxy-fuel cutting of steel

Master of Science Thesis

For the degree of Master of Science in Systems and Control at Delft University of Technology

Pooja Kumari

December 17, 2018

Faculty of Mechanical, Maritime and Materials Engineering (3mE) · Delft University of Technology

The work in this thesis was done in collaboration with HGG Profiling Specialists. Their cooperation is hereby gratefully acknowledged.

TU Delft Delft University of Technology

DCSC

Abstract

Oxy-fuel gas cutting is the most widely applied industrial thermal cutting process due to its various benefits such as low cost equipment, versatility and flexibility in terms of manual or mechanized operation. It is employed in cutting mild steel plates with thicknesses ranging from 0.5mm to 250mm, to manufacture heavy equipment such as windmills, offshore structures and structures in high-rise buildings.

In the cutting process, a mixture of oxygen and the fuel gas (here acetylene) is used to preheat the metal to its *ignition* temperature which, for steel, is 700°C - 900°C (bright red heat) but well below its melting point (1400°C). A jet of pure oxygen from the cutting torch is then directed into the preheated area instigating a vigorous exothermic chemical reaction between the oxygen and the metal to form iron oxide (slag in general term). The high pressure oxygen jet from cutting torch blows away the slag enabling the jet to pierce through the material and continue to cut through the material as the torch progresses.

Now, in order to optimize and automate this cutting process of steel, we will be studying various factors such as speed control of the cutting torch to maintain an accurate angled cut, need of preheater to improve quality of cut, the oxygen pressure required to enable the exothermic process sustained and to pierce deeper. Hence to study and implement the above factors, we need to have the knowledge of temperature distributions in the process at any stage.

The objective of the project is to obtain a dynamic model of the oxy-fuel gas cutting process by employing system identification techniques. The integral part is the study of heat transfer dynamics of the process and investigation of the parameters important in oxy-fuel cutting. Furthermore, we choose to model the heat sources in oxy-acetylene flame cutting, and the heat conduction in the steel using a numerical simulation based on the **Cell Method**. The cell method aims at numerical formulation of physical theories from the very outset, i.e. without discretizing the differential equations [1] and hence it is suitable for direct computer implementation. It requires the examination of parameters that are important when cutting different tubes and to develop a control system to automate the entire process with the aim of achieving improved cutting speed and high quality cut.

Table of Contents

List of Figures

List of Tables

Acknowledgements

It all started few years back, with the dream to pursue my higher education in an esteemed university with an intention to evolve myself holistically and grow personally and professionally. And here I am just a few days away from my graduation and accomplishing my dream. But this journey was nothing short of a roller coaster ride and I have quite a lot of people to thank without whom relentless support this would not have been possible. However, here, I will be extending my sincere gratitude to those people who helped me traversing my master thesis, a milestone of this journey which seemed unassailable.

The project is a vision of HGG and I am thankful to them and consider myself as a very lucky individual as I was provided with an opportunity to be a part of it and work on it as my thesis. It was a great chance for learning and professional development. I greatly appreciate the freedom they provided me to explore with their financial and logistical support and also the necessary guidance concerning projects implementation.

I thank my thesis supervisor prof. Dr. R. (Riccardo) Ferrari for providing invaluable guidance throughout my thesis. His door to office was always open whenever I ran into a trouble spot or had a question about my research or writing.

I express my warm thanks and deep gratitude to Mr. Matthijs for his incessant support and guidance at HGG. His expertise, experience and technical support served as the backbone in the implementation. I am thankful for all his aspiring guidance, invaluably constructive criticism and friendly advice during the project work.

Finally, I must express my very profound gratitude to my parents, siblings, friends and my husband for providing me with unfailing support and continuous encouragement throughout my years of study and through the process of researching and writing this thesis. This accomplishment would not have been possible without them.

I have deep gratitude to all those who has directly or indirectly provided me strength and motivation throughout this journey.

Delft, University of Technology — Pooja Kumari
December 17, 2018

Chapter 1

Introduction

Steel has a major influence on our day to day lives, from being the green choice for wind energy owing to its strength, flexibility, durability and 100% recyclable, to its use in energy efficient high rise buildings we work and live in. There are countless other facets of steel explaining clearly its undoubted benefits.

1-1 Background

The steel to be utilized for various purpose needs to be cut accurately and effectively to meet the requirement of the industry. Manual operations fails to produce very effective and consistent quality product. Also, since steel cutting requires precision, highly skilled labour is difficult to find and training them to accomplish the task is not cost effective. We can also not neglect the health hazard associated with these operations like excessive noise, toxic fumes and gases produced and the injuries caused due to hot metal slag and spatter. Hence, comes the need to automate the whole process of steel cutting in order to achieve very accurate cut with least amount of people involved. Automation aims to increase manufacturing efficiency and profitability for businesses that are tasked with repeatable production or rely on high-quality cuts or welds. When implemented, automated cutting yields improved quality and output of production processes, all while decreasing scrap and labor costs traditionally attached to manual operations.

There are many methods employed to cut steel depending upon the thickness and contour of the metal and cut. Few of them are Plasma Arc cutting, Laser Beam cutting, Oxy-fuel cutting etc. Oxy-fuel cutting is preferred over others as plasma cutting becomes prohibitively slow and expensive after a certain cut length and also it can not do bevel over 45°C. Also, oxy-fuel cutting is the most cost effective and can be used to sever metal of greater thickness and attain complex designs.

Oxy-fuel cutting as shown in figure 1-1 is a combustion process using oxygen/fuel gas (here acetylene) flame. There are two sources of heat, the preheater and the burner. The preheater brings the material up to its ignition temperature. And the jet of high pressure stream of

oxygen at least 99.5% pure from the burner is injected onto the heated spot through the torch. As the oxygen jet oxidizes the metal the torch is moved along the intended cutting path and a narrow kerf is created. The further supply of heat is provided by the heat generated in the exothermic reaction of the burning steel and the flow of heat through the process of conduction.

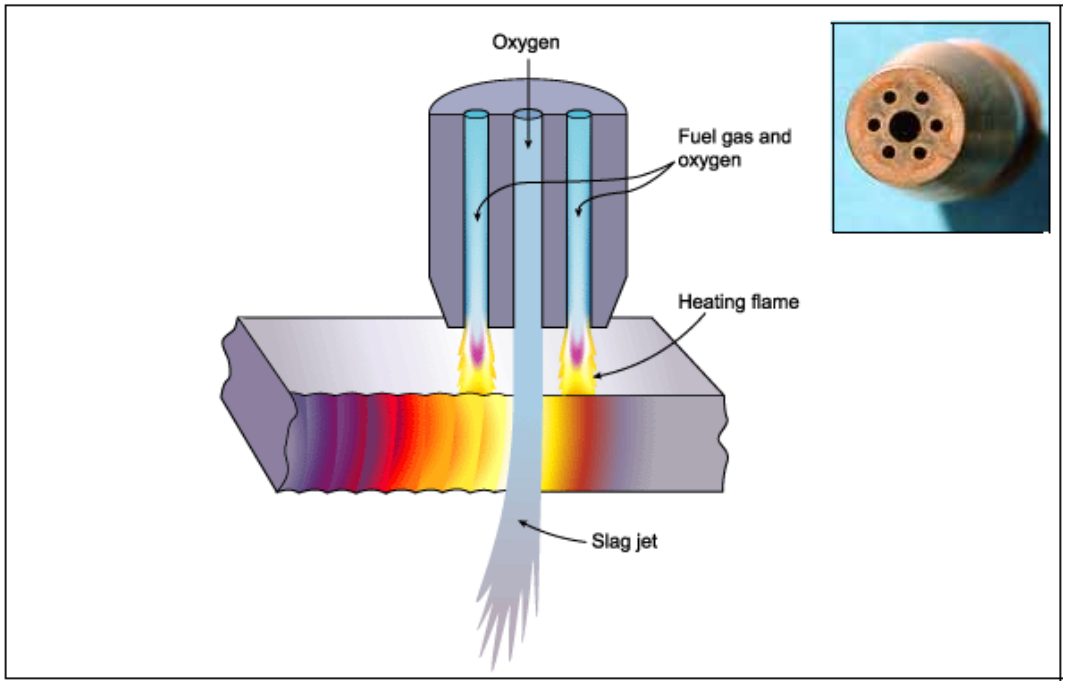

Figure 1-1: Diagram of oxy-acetylene cutting process and the nozzle design [2]

The basic requirements for oxy-fuel gas cutting are stated below [2]:

1. The ignition temperature of the material must be lower than its melting point otherwise the material would melt and flow away before cutting could take place (Figure 1-2).
2. The oxide melting point must be lower than that of the surrounding material so that it can be mechanically blown away by the oxygen jet.
3. The oxidation reaction between the oxygen jet and the metal must be sufficient to maintain the ignition temperature.
4. A minimum of gaseous reaction products should be produced so as not to dilute the cutting oxygen.
5. The thermal conductivity must be low enough so that the material can be brought to its ignition temperature.

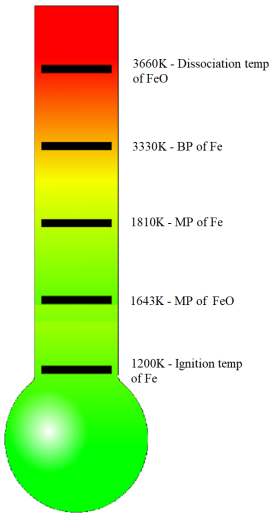

Figure 1-2: Temperature specs of mild steel (major content Fe) involved in cutting

Above the melting point of the metal, the viscosity of the oxidized melt should be lower than the metal itself, so that we get a cut which is free from re-solidified melt or dross along the bottom of the cut edge. Figure 1-3 shows that above the MP of Iron (which is 1810 K), the viscosity of FeO is lower than Fe, and hence FeO is easily removed from the cut zone creating a smooth cut.

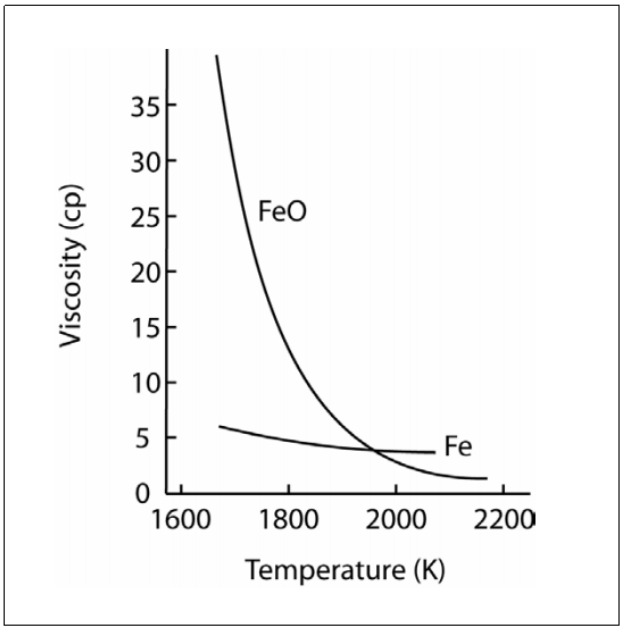

Figure 1-3: The relationship between viscosity and temperature for iron and FeO above 1900 K. [3]

The quality of the cut is determined by a number of variables like:

- the surface condition of the material (e.g temperature) and thickness of the material,
- size and design of the cutting tip,
- pressure and volume of the gasses,
- cutting velocity.

The figure 1-4 depicts the heat losses in the form of heat conduction to the surrounding metal, heat carried away by the molten slag/steel and and by the gases flowing out during the process.

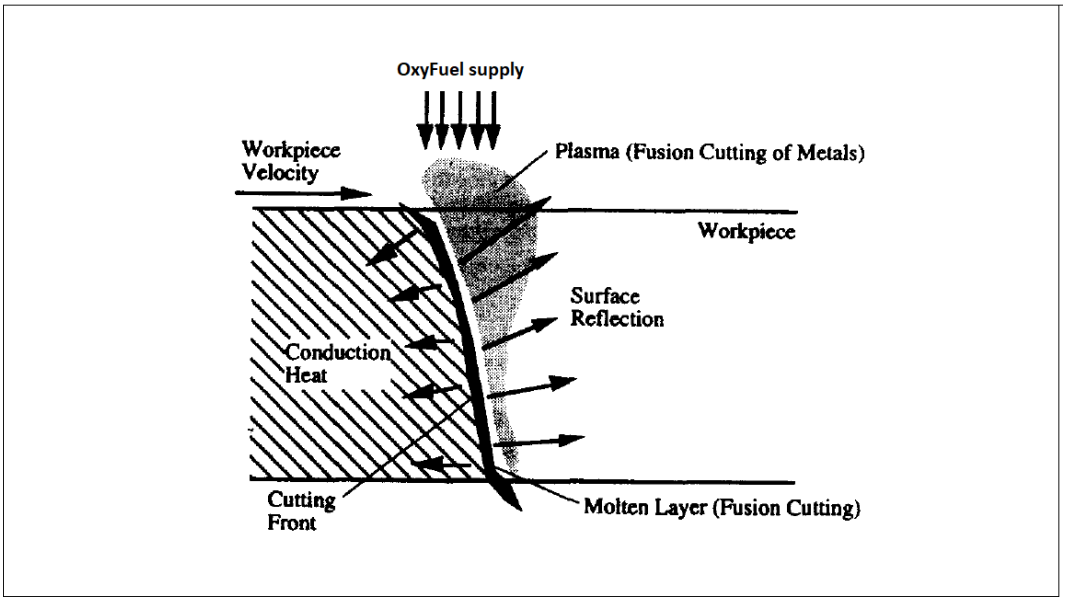

Figure 1-4: The heat transfer during oxy-fuel cutting [4]

1-2 Motivation

The main motivation of this project is to facilitate the oxy-fuel steel cutting process to be more mechanized i.e automated thereby implying less reliability on the human operators. The advantages associated with automated steel cutting are enormous in the form of consistent and improved cut quality, increase in production rate of the cut steel and efficiency. Also, labor is a major factor when considering the shift to automated cutting. Training individuals is a long-term and costly undertaking. Automated cutting also ensures labor and machine safety.

Now in order to achieve the goal of facilitating automation in the aforementioned steel cutting process, a complete information on the heat transfer and resulting temperature distributions

in the steel plates during the cutting process is significant. It is difficult to examine the thermal effect during oxy-fuel gas cutting because both the heat transfer between the gas flame and the work-piece and the exothermic reaction between the oxygen and the iron arise. The reason for taking up this project is due to the fact that it is challenging and interesting. Although bits of the concepts used in this project have been researched [5, 16, 17, 18]. However, the model of the heat source and thermal analysis of the overall phase transition in the oxy-fuel cutting in order to facilitate the design of control systems have not been done before. This makes the project very stimulating and useful.

Chapter 2

State of the art

2-1 Fundamentals

Oxy-fuel cutting is the most widespread, relevant and accurate cutting technique used for the cutting of the mild steel. The basic principle is that when the metal is heated to a temperature of 900°C (depending on the type of alloy), it will burn if brought in contact with oxygen. If it comes in contact with the oxygen of the surrounding air only, then combustion will occur only on the surface of the metal. However, if a jet of pure oxygen under high pressure is directed at the hot metal, the metal will burn through a narrow zone, called a kerf.

In the oxy-fuel cutting, the steel being cut is usually a low carbon grade. This is an alloy of iron (99% by weight), carbon (0.05% to 0.25% by weight) and the rest is other elements like silicon, manganese, and phosphorus, depending on the ore used. The steel is preheated to the ignition temperature by the oxy-acetylene flame directed through the preheater. The steel loses all the protective properties (layers of oxides formed on the surface of steel to prevent from rusting) against oxygen and is still solid. Pure oxygen under high pressure is then directed through the nozzle at the heated area. This fine jet of oxygen transforms the pre-heated steel into the oxidized liquid steel/slag by an exothermic reaction. The iron content of the steel is oxidized to iron oxide while the carbon transforms into carbon monoxide. This oxide of steel has lower melting point than steel, and gets blown out of the kerf by the the oxygen stream without affecting the non-oxidized solid steel. This exothermic reaction is a continuous process and creates a cut as the torch moves. To keep the exothermic reaction working, the cutting torch keeps the steel heated during cutting. Only metals whose oxides have a lower melting point than the base metal itself can be cut with this process. Otherwise as soon as the metal oxidizes it terminates the oxidation by forming a protective crust [19]. In order to achieve a continuous operation there must be a balance among the speed of the movement of the cutting torch, oxygen jet size, and the intensity of flame.

The phase transformation stages involved in the cutting process is illustrated in figure 2-1. The kinetics of oxidation reactions of metals at high temperatures are assumed to be controlled by the rates of mass transport of reactants and products in the gas-slag interface,

slag-metal interface and slag phases [20]. The sources of heat which provides energy for the smooth transitioning of the complete process are the ones generated by the oxyacetylene combustion, the oxidation of Iron and Carbon present in the steel at the slag-steel interface and the Carbon monoxide (which is the product at slag-steel interface) oxidation with the excess oxygen at the gas-slag interface [21]. The basic processes which are involved in flame

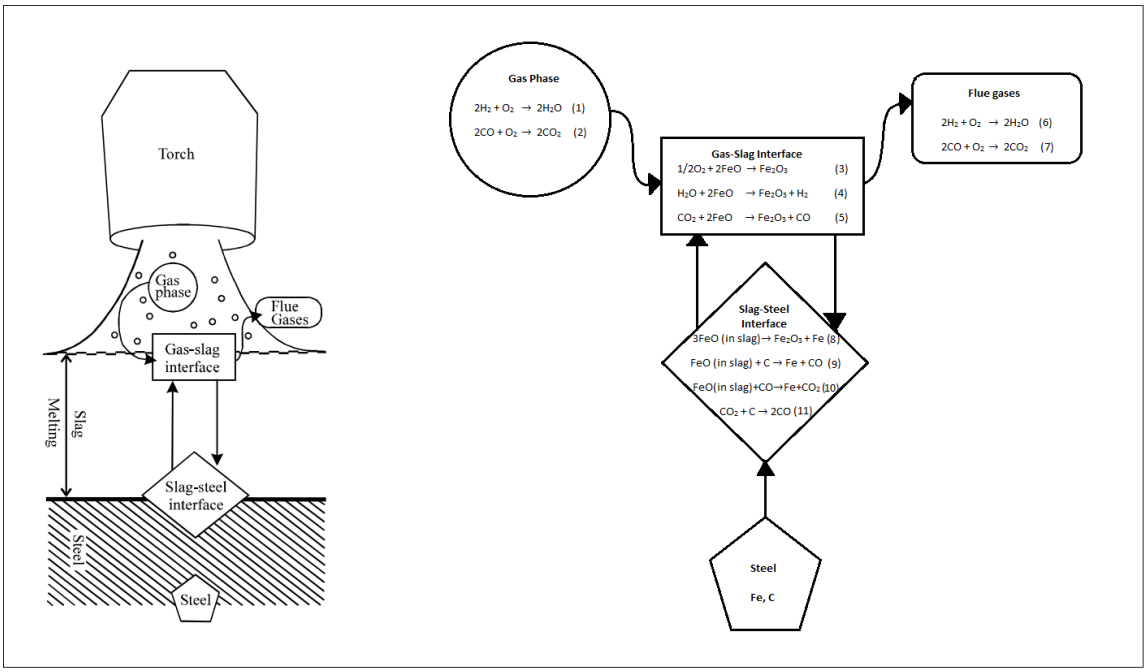

Figure 2-1: The Phase transformation stages of the oxy-fuel steel cutting process (adapted from [5])

.

cutting are described below [5]:

- *diffusion and collision of gas molecules and/or atoms with the metal*
- *adsorption kinetics of the reactants to the surface of the metal*
- *reaction at the surface*
- *desorption kinetics of products from the surface*
- *diffusion of products away from the surface*

2-2 Literature Review

In this section we are going to elucidate the existing research and the papers pertaining to the concepts required in finding the solutions of the project. Also their goals and contributions and relevance to this project is studied. Section **2-2-1** deals with the kinetics of the reactions/ process, which studies the rates of reaction involved in the oxy-fuel gas cutting process.

Section **2-2-2** deals with the thermodynamic analysis of the cutting process. Section **2-2-3** deals with the numerical approaches for the heat flow modelling.

2-2-1 Kinetics of Oxyfuel gas cutting of Steel

Kinetics is the study of rate of reactions in the chemical process. In the oxy-fuel gas cutting the basic process lies in the rapid high-temperature oxidation of the cut metal.

The principle of oxyacetylene cutting is that when metal is heated to its ignition temperature by oxyacetylene flames and a jet of pure oxygen is directed at the hot metal, a chemical reaction known as **oxidation** takes place. When oxidation occurs rapidly, it is called **combustion** or **burning**; when it occurs slowly, it is called **rusting**. When metal is being cut by the oxyacetylene torch method, the oxidation of the metal is extremely rapid i.e. it burns. The heat liberated by the burning of the iron or steel melts the iron oxide formed by the chemical reaction, and it also heats the pure iron or steel [5]. The molten material runs off as slag, exposing more iron or steel to the oxygen jet.

Oxyacetylene Combustion:

The oxy-fuel cutting process requires a preheat flame which is fuel gas mixed with pure oxygen and then ignited by the outside spark or flame. After the ignition of the flame, the initial spark is withdrawn and the burning flame becomes the heat source that ignites the fuel oxygen/fuel gas mixture that continues to flow from the nozzle. The complete combustion of acetylene takes place in two stages [6].

The first stage uses the oxygen supplied from the nozzle of the cutting torch in the preheating. Here, the oxygen combines with the carbon of the acetylene to form carbon monoxide (CO), while the hydrogen (H_2) is liberated [22]. This reaction can be seen as the small inner cone of the flame which is at the highest temperature.

$$2C_2H_2 + 2O_2 \rightarrow 4CO + 2H_2 + heat \tag{2-1}$$

The second stage uses the oxygen supplied from the air surrounding the flame. The carbon monoxide takes up oxygen from the atmosphere, and as a result of burning forms carbon dioxide (CO_2). The hydrogen also burns with oxygen from the atmosphere to form water vapour (H_2O). This combustion zone constitutes the outer envelope of the flame.

$$4CO + 2H_2 + 3O_2 \rightarrow 4CO_2 + 2H_2O + heat \tag{2-2}$$

The overall chemical equation for the complete combustion of acetylene is shown below:

$$C_2H_2 + \frac{5}{2}O_2 \rightarrow 2CO_2 + H_2O + 1309.5kJ/mol.[8] \tag{2-3}$$

Combustion of oxygen and acetylene, when combined in proper proportions, yield a flame with a temperature of about 3480 °C (Figure 2-2) and 1309.5 kJ/mol heat is generated.

The chemical action of the oxyacetylene flame can be adjusted by changing the ratio of the volume of oxygen to acetylene. Three distinct flame settings are used, **neutral, oxidizing**

and carburizing (Figure 2-3). The neutral flame has a one-to-one ratio of acetylene and oxygen[23]. It obtains additional oxygen from the air and provides complete combustion. The oxidizing flame is obtained by increasing just the oxygen flow rate while the carburizing flame is achieved by increasing acetylene flow in relation to oxygen flow. As deduced from figure 2-4, for maximum flame efficiency, oxygen and acetylene should be premixed in the ratio of at least 1.7 to 1 and oxygen and propane in the ratio of 4.5 to 1 [7] i.e. the flame should be oxidizing. When applied to steel, an oxidizing flame causes the molten metal to foam and give off sparks. This indicates that the excess oxygen is combining with the steel and burning it.

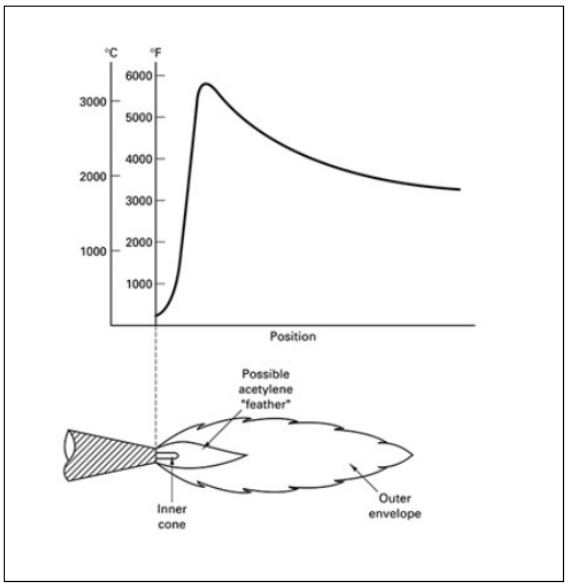

Figure 2-2: Typical oxy-acetylene flame and the associated temperature distribution [6]

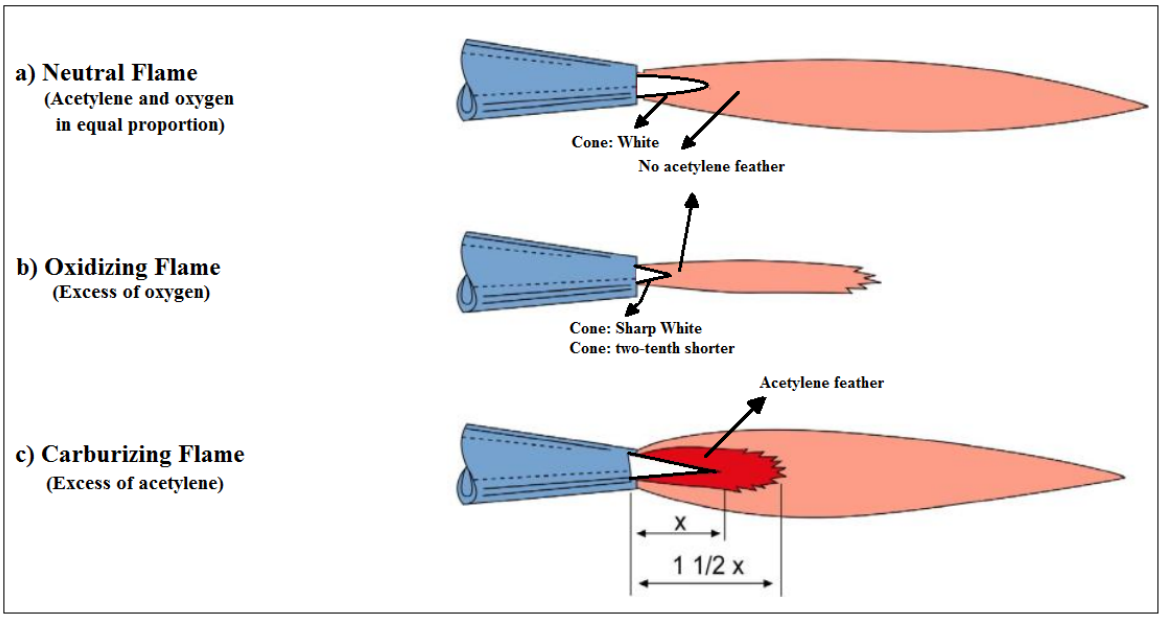

Figure 2-3: Oxy-acetylene flame types for cutting [6]

Metal Oxidation:

During the actual steel burning process, a jet of pure oxygen is being fed into the molten steel, feeding a rapid oxidation process, or "burning" of the steel. During this process, the chemical reaction of oxidizing steel is "exothermic", meaning that it gives off more heat than it takes to start the reaction. After the plate is preheated and the burning starts, the preheat flame is turned down to a lower setting. But the preheat flame continues to provide the heat & ignition source, while the cutting oxygen stream provides the oxidizer, and the steel itself is the fuel. Allowing for the loss of heat by radiation and conduction, there is ample heat to sustain the reaction.

Oxidation of steel at temperatures higher than 873K leads to multi-layer iron oxide formation consisting of wustite (FeO), magnetite (Fe_3O_4) and hematite (Fe_2O_3), in increasing order of oxygen content, going from substrate to free surface. The chemical reaction in iron and carbon combustion, by oxidation at ignition temperature of steel and the considerable heat liberated is shown below in Equations (2-4) to (2-8) [6]. The mass ratios of the oxides FeO/ Fe_3O_4/ Fe_2O_3 are typically 95/ 4/ 1 [5]. Wustite (FeO) is the predominant oxide in the oxidation reaction of iron.

$$Fe + \frac{1}{2}O_2 \rightarrow FeO \qquad +267kJ/mol \tag{2-4}$$

$$Fe + \frac{2}{3}O_2 \rightarrow \frac{1}{3}Fe_3O_4 \qquad +1120kJ/mol \tag{2-5}$$

$$Fe + \frac{3}{4}O_2 \rightarrow \frac{1}{2}Fe_2O_3 \qquad +826kJ/mol \tag{2-6}$$

$$C + O_2 \rightarrow CO_2 \qquad +393kJ/mol \tag{2-7}$$

$$C + \frac{1}{2}O_2 \rightarrow CO \qquad +99kJ/mol \tag{2-8}$$

TABLE 3-1a. COMBUSTION PROPERTIES OF OXYGEN-ACETYLENE

(Primary combustion of acetylene in inner-flame cone) *

Ratio, oxy./acet.	Type of flame †	Mol. vol of combustion products						Heat liberated		Flame temp, °F ‖
		C ‡	CO	CO_2	H_2	H_2O	O_2	Btu	% of total §	
0.8/1.0	Car.	0.4	1.60	0	1.00	0	0	173,000	31.7	5550
0.9/1.0	Car.	0.2	1.80	0	1.00	0	0	184,000	33.9	5700
1.0/1.0	Neu.	0	2.00	0	1.00	0	0	195,000	35.9	5850
1.5/1.0	Ox.	0	1.80	0.20	0.70	0.30	0.25	250,000	46.1	6200
2.0/1.0	Ox.	0	1.72	0.28	0.56	0.44	0.61	275,000	50.7	6100
2.5/1.0	Ox.	0	1.65	0.35	0.51	0.49	1.10	288,000	53.2	6000

* Based on 1 molecular volume of acetylene = 26.02 lb = 380 cu ft, at 60°F, and 1 atmosphere.
† Car. = carburizing, Neu. = neutralizing, Ox. = oxidizing.
‡ 0.4 molecular weights of solid carbon = 4.8 lb.
§ Total heat liberated for complete combustion of acetylene, 542,700 Btu per molecular volume.
‖ Theoretical. Actual flame temperatures are at least 10 per cent lower.

TABLE 3-1b. COMBUSTION PROPERTIES OF OXYGEN-PROPANE

(Primary combustion of propane in inner-flame cone) *

Ratio, oxy./pro.	Type of flame †	Mol. vol of combustion products					Heat liberated		Flame temp, °F §
		CO	CO_2	H_2	H_2O	O_2	Btu	% of total ‡	
1.5/1.0	Neu.	3.0	0	4.00	0	0	92,000	10.5	2100
2.0/1.0	Neu.	2.85	0.15	3.15	0.85	Trace	199,000	22.7	3500
2.5/1.0	Ox.	2.75	0.25	2.25	1.75	Trace	305,000	34.8	4700
3.0/1.0	Ox.	2.65	0.35	1.65	2.35	0.15	380,000	43.3	5200
3.5/1.0	Ox.	2.55	0.45	1.30	2.70	0.43	429,000	48.9	5300
4.0/1.0	Ox.	2.50	0.50	1.10	2.90	0.80	456,000	52.0	5400
4.5/1.0	Ox.	2.45	0.55	0.95	3.05	1.20	477,000	54.5	5300
5.0/1.0	Ox.	2.40	0.60	0.90	3.10	1.65	488,000	55.8	5200

* Based on 1 molecular volume of propane = 44.06 lb = 380 cu ft, at 60°F, and 1 atmosphere.
† Neu. = neutralizing, Ox. = oxidizing.
‡ Total heat liberated for complete combustion of propane, 876,000 Btu per lb molecular volume.
§ Theoretical. Actual flame temperatures are lower because of radiation.

Figure 2-4: Combustion properties of Oxygen-Acetylene and Oxygen-Propane [7]

In oxyacetylene cutting, only that portion of the metal that is in the direct path of the oxygen jet is oxidized. Thus, a narrow slit (called a kerf) is formed in the metal as the cutting progresses. Most of the material removed from the kerf is in the form of oxides (products of the oxidation reaction). The remainder of the material removed from the kerf is pure metal, which is blown or washed out of the kerf by the force of the oxygen jet. Since oxidation of the metal is vital part of the oxyacetylene cutting process, this process is not suitable for metals that do not oxidize readily, such as copper, aluminum, high alloy steel, and so on. Low-carbon steels are easily cut by the oxyacetylene cutting process.

Other factors:

Now, apart from the combustion of oxyacetylene and oxidation of metal, the kinetics of the process significantly depends upon other factors as well. The composition of the cut metal, the activities of the reactants and the commercial impurity of oxygen are to name a few that affects the rate of cutting steel.

Adedayo [5] studied the role of carbon on the kinetics of the process and also the effects of the activities of oxyfuel gases on the flame cutting process. He investigated the variations in cutting rate due to **1) the effects of carbon content of the steel on cutting rate at different acetylene pressures,** and **2) the effects of oxygen pressure on cutting rate for different carbon content of cut steels**.

For the experiment he used steel rods of different compositions and at the required pressures, cutting torch was used to heat the steel rods surface to ignition temperature (steel rod turns cheery red). Oxygen was then supplied to react with the metal and the formed oxide slag was flown out of the kerf by the kinetic energy of the oxygen stream. He used different acetylene and oxygen pressures to conduct the experiment. The time taken to cut the rods was noted and the cutting rate was calculated by finding the ratio of the diameter of rod to the total time taken. From the data obtained, he observed that there is a **decrease in cutting rates with increase in carbon content** as a result of reduction of iron oxide and carbon dioxide during decarburization reactions (Equations (2-9) to (2-11)) in the slag-steel and gas-slag interfaces. These reactions are unfavourable for the formation of FeO.

$$FeO + C \rightarrow Fe + CO \tag{2-9}$$

$$FeO + CO \rightarrow Fe + CO_2 \tag{2-10}$$

$$CO_2 + C \rightarrow 2CO \tag{2-11}$$

Hence, steels with high carbon density are more difficult to flame cut because of the reactions between carbon, carbon monoxide and iron oxide.

Also, kinetics of reactions are mainly controlled by the collision theory [24]. For any reaction to occur, the molecules are needed to collide with enough energy. And this is true whether both particles are in the gas state, or whether one is a gas and the other a solid figure 2-5. So if the pressure is higher, the chances of collision are greater therefore **cutting rates increase with the increased oxy-fuel pressure**.

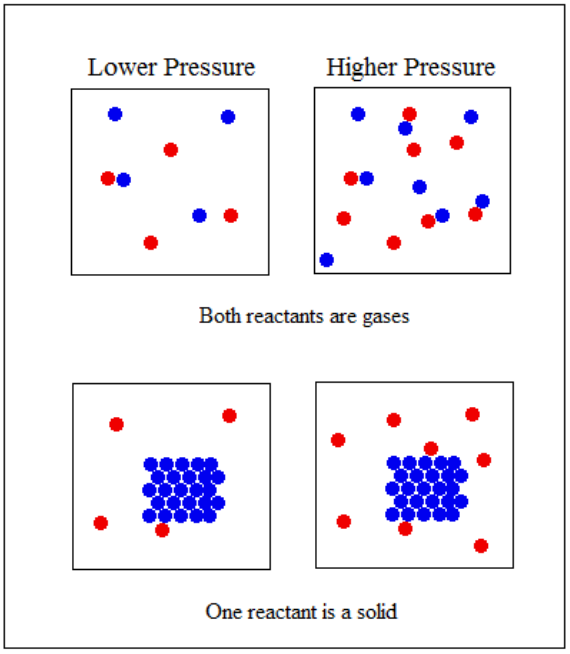

Figure 2-5: Collision of two particles at different pressures

The **commercial impurity of oxygen** being contaminated by other gases also affects the cutting speed. As demonstrated by the graph in figure 2-6, a decrease in oxygen purity of 1% will typically reduce the cutting speed by 25% and increase the gas consumption by 25% [8].
Discussion: Based on the study, we can deduce the below finding in the context of oxy-acetylene cutting of steel:

- *Finding 1:* During the oxyacetylene cutting of mild steel the oxidation reaction of iron to FeO supplies a considerable amount of energy to the cutting process.
- *Finding 2:* The thermal energy provided to the cutting process by the oxidation reaction is approximately 250 kJ/mol.
- *Finding 3:* Not all the iron melted during cutting is oxidized, the melt leaving the cut is the mixture of Iron and Iron oxide.
- *Finding 4:* The cutting rate is decreased with the increase in carbon content and increased with increase in the oxy-fuel pressure.
- *Finding 5:* When flame cutting, the preheating flame should be neutral or oxidizing . A reducing or carbonizing flame should not be used.

These results will help in the modelling of the heat source and heat flow in the steel considering the heat energies associated with the hot gas in, hot gas out plus the slag and the chemical reactions in the process.

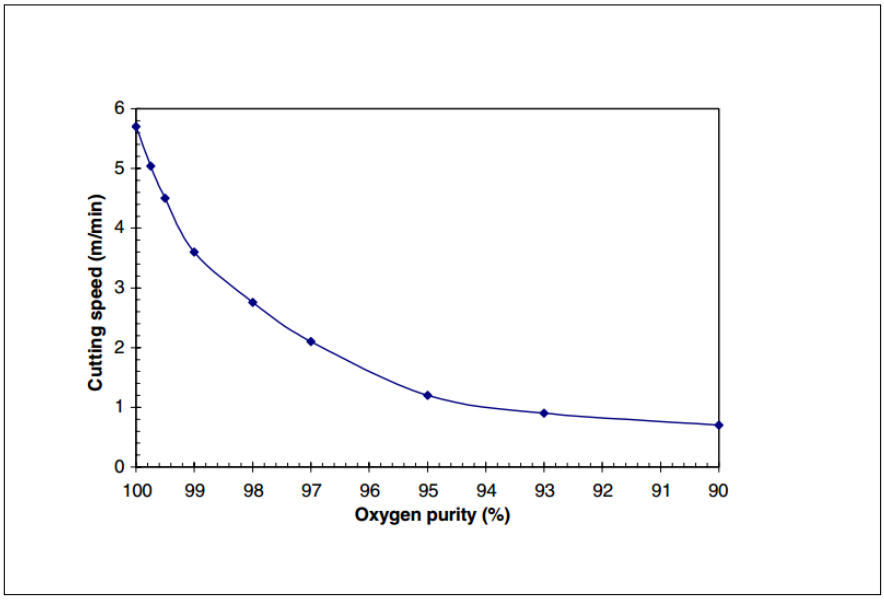

Figure 2-6: Cutting speed as a function of oxygen purity [8]

2-2-2 Thermodynamics of Oxy-fuel gas cutting of steel

Thermodynamics is the study of heat and temperature and their relations to other forms of energy (chemical here). How can we measure heat? Here are some things we know about heat so far:

- When a system absorbs or loses heat, the average kinetic energy of the molecules will change. Thus, heat transfer results in a change in the system's temperature as long as the system is not undergoing a phase change.
- The change in temperature resulting from heat transferred to or from a system depends on how many molecules are in the system.

Next comes the question, How can we use the change in temperature to calculate the heat transferred? Now, in order to analyze this we need to know few factors in the context of oxy-fuel cutting like,

- the total heat liberated in the reactions of elements and oxygen
- the specific heat of the materials and of the combustion products
- the melting point of the materials and of the oxides formed
- the thermal conductivity of the materials and of the oxides

- the heat of fusion of the material
- the rate of diffusion of the oxygen through the combustion products to the cutting zone
- the viscosity of the combustion products and their rate of removal from the cutting face
- the rate of reaction of oxygen with the material at the cut face under varying rates of oxygen supply at various pressures and temperatures

Figure 2-7 shows the different interfaces of the phase transformation in the oxy-fuel steel cutting describing the source and state variables in different phases and the corresponding heat energy of the system. The black box describes the stages and the green boxes are the interfaces between the two successive stages. Once the cut has started and steel has reached the ignition temperature, then the jet of high pressured oxygen is used for the metal oxidation [25]. Now the heat is utilized in the phase transformation of solid steel to molten steel, oxidation of solid steel to form slag and phase transformation of solid carbon to carbon monoxide and carbon dioxide gases, in the slag-steel interface. When the further oxygen is supplied to the oxidized metal, which is in molten phase, most of the slag is blown out creating kerf and the carbon monoxide and carbon dioxide is flown out to the atmosphere.

There are a very few works in the literature which address the thermodynamics involved in the Oxy-fuel Gas cutting in general. Powell [3] studied the thermodynamics of the Iron to FeO oxidation reaction in the context of laser-oxygen cutting of mild steel. In principle, the laser-oxygen cutting process is similar to the flame cutting, which involves preheating the metal to the required ignition temperature using an oxygen and fuel gas flame/ laser-oxygen thereby initiating and propagating an exothermic oxidation reaction between oxygen and iron which provides sufficient energy to the cutting process and also generates a low viscous, oxidized melt which gets removed by the supply of stream of high purity oxygen into the cut zone. The paper focuses on the analysis of the energetic contribution of the oxygen reaction to the cutting process as a function of temperature and oxygen pressure. And it concluded that *The thermal energy provided to the cutting process by the oxidation reaction is approximately 250 kJ/mol.* But the literature only considered the thermal energy provided by the oxidation of iron to FeO and **did not consider the heat energy provided by the laser input**.
During oxy-fuel cutting, the cutting flame heats the metal to start the process and the further considerable amount of heat is provided by the exothermic reaction of the burning metal. These heat sources are considered as heat input (Q). The energy associated with the chemical reaction, i.e. change in Gibbs Free Energy(ΔG) is given by,

$$\Delta G = \Delta H - T\Delta S \tag{2-12}$$

where, ΔH is change in enthalpy i.e. heat energy evolved by the reaction, T is the temperature in K and ΔS is the change in entropy. ΔG and ΔH are temperature dependent.

$$\Delta H_{T2} = \Delta H_{T1} + \int_{T1}^{T2} C_p dT \tag{2-13}$$

where, C_p is the specific heat capacity at constant pressure [3].

The total heat input Q is given by the sum of heat liberated by eqs. (2-3), (2-4), (2-7) and (2-8). The relationship between the total heat input and final reaction temperature (T_f) is

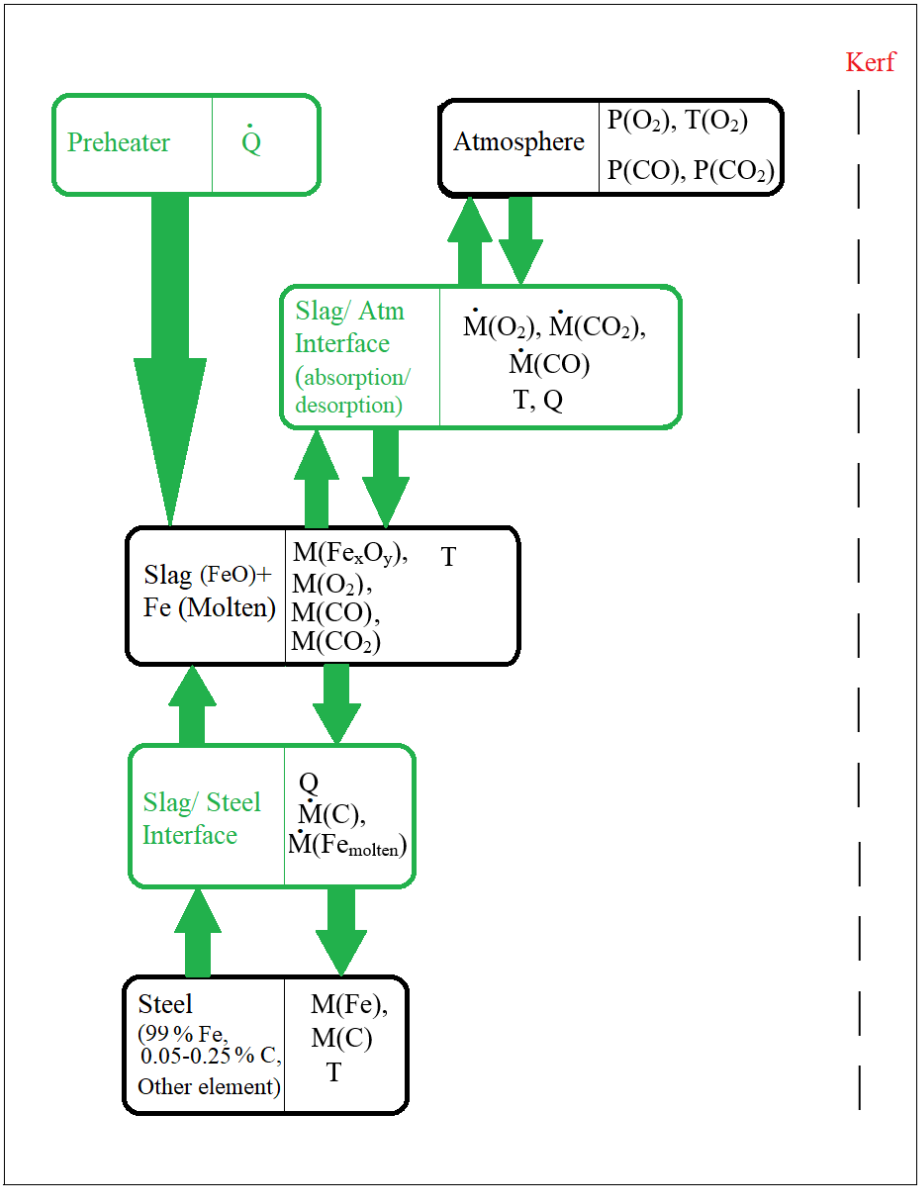

Figure 2-7: The Phase transformation stages of the oxy-fuel steel cutting process.

expressed as:

$$Q = \int_{298}^{T_f} \sum n_i C_{p(product)} dT \tag{2-14}$$

Where C_p is the specific heat capacity of products (FeO, CO_2, CO, H_2, H_2O) at constant pressure, n_i is the mole fractions of component i in the product.

Now, from the given values of heat liberated by eqs. (2-3), (2-4), (2-7) and (2-8), if we calculate the total heat (Q), it will be approximately, 2068.5 kJ/mol (though this might vary as per the mole fractions of component in the product obtained). And the latent heat of fusion of main components of steel, which is iron slag and carbon is 13.8 and 105 kJ/mol. So, the total

118.8 kJ/mol(plus some more heat for the other minor components in the alloy of steel) heat energy is utilized in the phase transformation in the slag steel interface.

The total value of Q depends on the ratios of n_{FeO} : n_{CO_2}: n_{CO} . This ratio is a function of concentration and activity of carbon and oxygen. According to [3], there is increased tendency for formation of carbon dioxide at lower carbon . Since $C_{p(CO2)}$ is about twice the value of $C_{p(CO)}$, higher values of n_{CO2}: n_{CO} will give higher heat input.

Though there will be considerable amount of heat loss due to heat loss by the molten slag and the reduction reaction of Iron oxide and carbon dioxide, still there is major amount of heat present which is conducted in the metal and provides the energy necessary to keep the reaction going and aids the cutting process.

Also, as stated in [3], the cutting rate increases with increase with temperature. This can be explained as, once we accelerate the cutting process we need to transport heat more quickly to the melt/solid interface. This means that the thermal gradient must become steeper which means that the temperature of the melt surface must increase. This inference was drawn for laser-oxygen cutting. But in case of oxy-fuel cutting the behaviour might not be the same. The higher temperature will melt more Fe with FeO and we might land up getting distorted kerf.

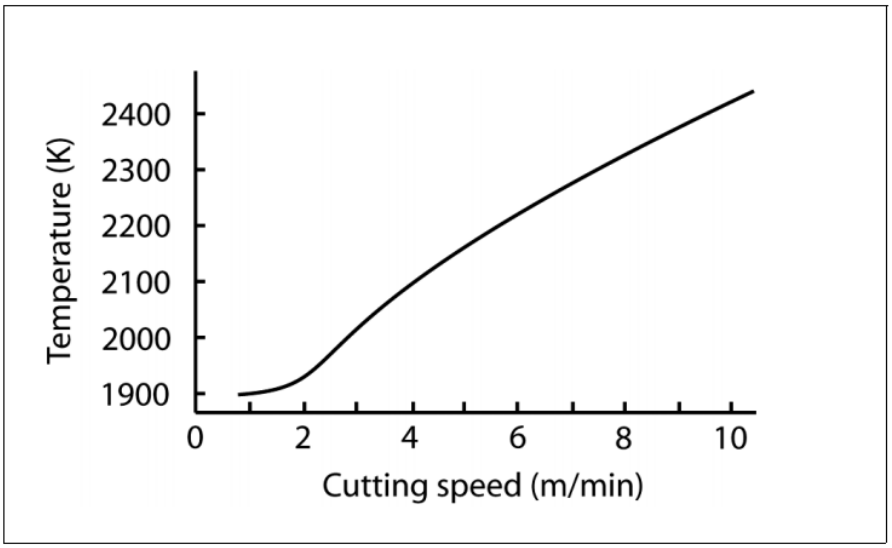

Figure 2-8: Relationship between cut front temperature and cutting speed [3].

Discussion: After the study of thermodynamics of the oxy-fuel cutting, we can draw the inference that there is sufficiently high heat energy evolved during the cutting in order to sustain the whole process. Also cutting mild steel with oxygen at moderate or high speeds, the cut front temperature will rise as a function of the cutting speed. This is a significant factor in modelling heat transfer, as it will influence the conduction speed of heat.

2-2-3 Numerical modelling of heat flow and temperature distributions

The oxy-fuel steel cutting process is very complex since it involves simultaneous multi-phase solid/gas/liquid interactions, chemical reactions, heat and mass transfer and complex flow patterns at high temperatures as shown in figure 2-1. The transient nature of the process also adds more complexities and the severe operating conditions inhibit the direct measurement and observation of the process. This difficulty can be addressed by developing models, which makes it possible to describe the complicated nature of the process itself and to understand the interconnection of important process variables.

A literature survey has revealed only a limited number of publications on the numerical modelling of heat flow and temperature distributions in the steel cutting process. In the 1940s, Rosenthal [26] proposed a mathematical approach for the heat distribution during welding and cutting by using a combination of heat point sources. In order to find analytical solutions, the medium was considered as semi-infinite and thermophysical properties were assumed to be constant. Since the temperature of steel changes from room temperature to melting point in a short interval, therefore its not appropriate to have linear approximation in which the temperature dependence of thermophysical properties is assumed constant. The study did not consider the phase change effects and the latent heat effects were ignored. It also neglected property gradients, e.g., the variation of thermal conductivity with temperature which is an important factor is determining the thermal histories and analyzing suitable cutting speed.

Concerning flame cutting per se, the oxyfuel gas cutting process was studied by Adedayo [5] who reported different chemical reactions taking place in the flame cutting and also studied the effect of oxy-fuel pressure on the kinetics of the process. But it did not mention any heat associated with these reactions.

Terasaki [9] experimentally investigated the heat input generated and it's distribution along the thickness in plate by gas cutting process. They proposed a model of heat input that take into account the preheating flame, the oxidation reaction and dross(figure 2-9). They assumed heat input distribution of the preheating flame as gaussian distribution. In order to measure the effective amount of heat on the metal, we need to consider the effect of radiation and the heat transfer due to conduction. But they did not considered these effect. This is the major flaw in the correct estimation of heat input. Also, they did not do thermal heat flow analysis of the process.

Osawa [10] studied the heat transfer during the piercing process in order to be able to automate the preheating flame. But because of the thermal complexities of thermal effect during flame cutting, the relation between the preheating flame conditions (fuel gas, gas conditions, the total calorific value, etc.) and the cutting performances (cutting speed, kerf quality, thermal distortion, etc.) are difficult to estimate. Hence they developed a genetic algorithm (GA) based heat transfer estimation technique which can be applied to cases where the heating face temperature exceeds the ignition temperature of steel. Using GA they identified the heat transfer parameters, the local heat transfer coefficient, α, and the gas temperature adjacent to the plate, T_G. And using these identified variables they calculated the piercing process and the piercing performance was estimated by calculating the time until the plate face temperature reaches the kindling temperature. The validity of the proposed piercing performance estimation method was examined by comparing the estimated and measured minimum piercing times. The plot in figure 2-10 is measured(rhombus for LPG and plus for

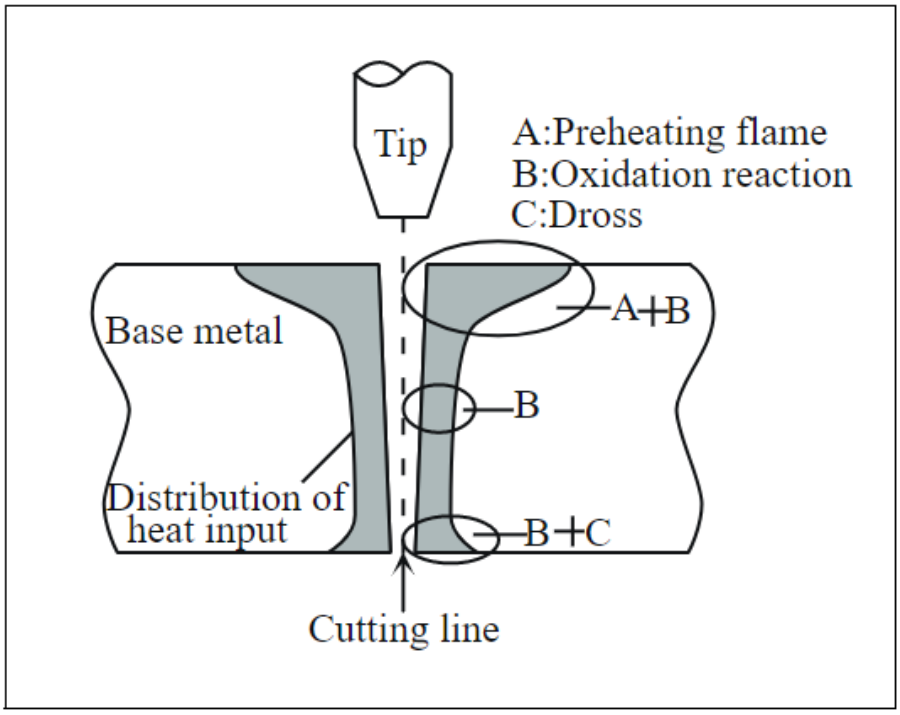

Figure 2-9: Model of heat Input by Terasaki [9].

H_2/LP fuel gas) for the heat test at the distance of r=6mm from the spout of the preheater and compared with the ones calculated(dotted line for LPG and straight line for H_2/LP fuel gas). The measured data show fluctuations and it could be due to changes in plate surface condition. The result are interesting but the approach of using GA based heat transfer estimation is incomprehensible from an engineering point of view. It works on black-box approach that work amazingly well to describe data but provide little to none understanding of generating mechanisms. The time taken to for convergence is unpredictable. For a heavy simulation, it can often take days for a solution. Also, the results obtained can not be extended to other settings.

Lindgren [27] assumed the steady state heat flow for the simulation of flame-cutting of steel plate. He did the thermal analysis of the heat flow using Finite Element Model(FEM). He modelled a 2D section with x-axis transverse to the cutting direction and the y-axis along the thickness of the plate. And the heat flow in the cutting direction (z-axis) was assumed to be negligible as the cutting speed was relatively high. The thermal analysis was also simplified by assuming symmetry along the mid-surface of the plate, i.e., the xz-plane was a symmetry plane. Thus, only the upper half of the plate was analyzed. These assumptions do not provide the holistic modelling of the heat input as there will be significant heat flow in the complete steel plate due to conduction which will be influential in causing the residual stresses. Also the oxidation reaction between iron and oxygen heats the cutting line through the thickness, and even the molten droplets heat some parts on the lower surface near the cutting line which was not included in determining the heat input.

Bae [11] studied the numerical analysis of heat flow in oxy-ethylene flame cutting of steel

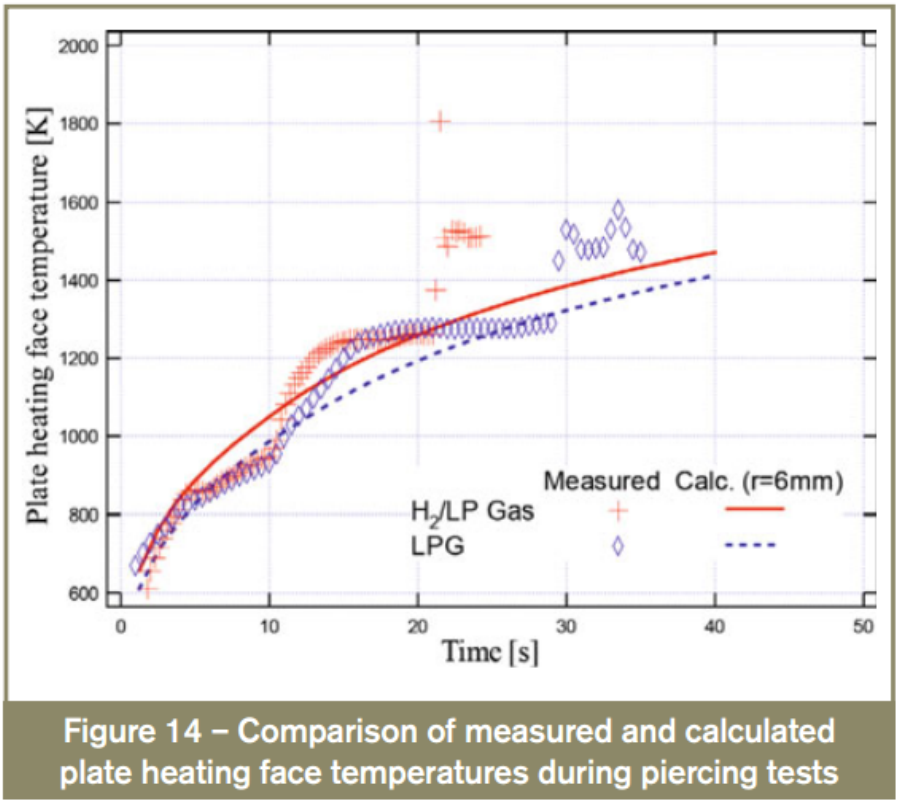

Figure 2-10: Comparison of measured and calculated plate heating face temperatures during piercing tests using GA [10].

plate. He proposed the heat source model consisting of three parts: (1) the heat flux on the upper surface, (2) the reaction heat at the cutting line, and (3) the heat from the droplets on the lower surface. And the heat flow analysis was performed by the numerical simulation using the finite element method (FEM). As [27], he also considered that the cutting speed was much faster than the conduction speed of heat, therefore a quasi-steady state was assumed. Hence, a 2D analysis was performed on the midsection of the steel plate with a unit length to estimate the temperature histories of each position on the section.

Figure 2-11 shows the 2D model of heat source. The heat sources consist of a flame heating on the upper surface of the plate, reaction heating between oxygen and heated iron along the cutting line through the thickness(x-axis), and heat conduction from the molten droplets to the lower surface near the cutting line(y-axis). The heat flow in the midsection with unit length of the plate, represented as the solution domain was analyzed by the heat sources, as the cutting torch traveled along the cutting direction.

The shape of flame was modelled using a Gaussian distribution, the equation being,

$$q_1(r) = \frac{3\eta Q_1}{\pi \bar{r}^2} e^{-3(\frac{r}{\bar{r}})^2} \tag{2-15}$$

where $q_1(r)$ is the heat flux at a position r, $\bar{r}$ is the effective radius of heat flux(35mm), Q_1 is the heat of enthalpy due to oxy-ethylene combustion which is 14.152 kcal/L and η is the

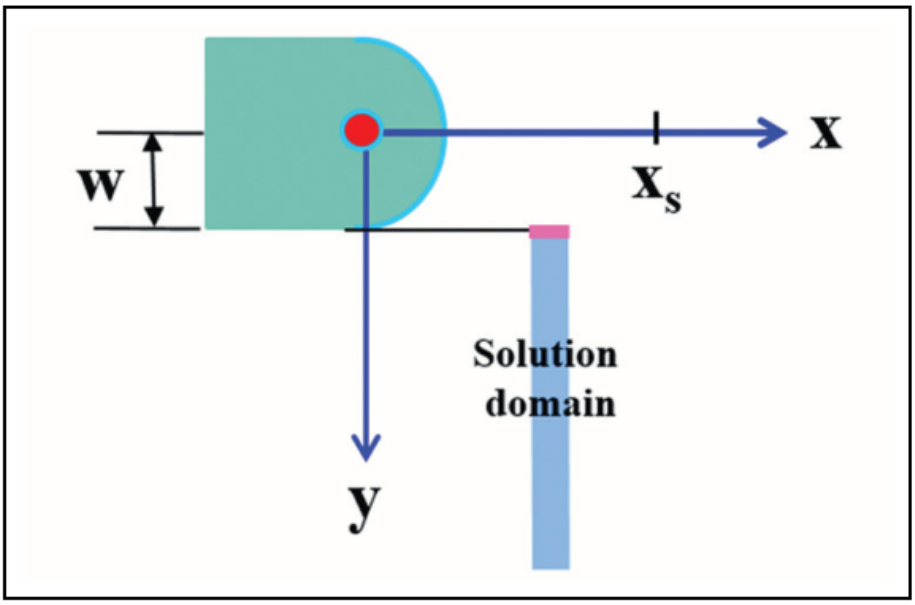

Figure 2-11: Heat source and solution domain [11].

efficiency of oxy-fuel flame which was assumed to be 0.5. Now, when the heat source due to the iron oxidation reaction along the cutting line approaches the melting temperature of the oxidized iron, the temperature along the cutting line of the solution domain increases. For the estimation of heat generated on the line due to varying time, the RosenthalâĂŹs analytic solution for the temperature distribution on an infinite plate with the line heat source on the plane transverse to the cutting direction was considered. The governing equation for the analytic solution for temperature T at a location with coordinates in the x and y axis with the heat source Q_2 moving at a speed of v being,

$$T - T_0 = \frac{Q_2}{2\pi dk}\sqrt{\frac{\pi\alpha}{vR}}e^{-\frac{v(x+R)}{2\alpha}} \tag{2-16}$$

where $R = \sqrt{x^2 + y^2}$, x and y are coordinates of a location, T_0 is the initial temperature, d is the thickness, k is the thermal conductivity, and α is the thermal diffusivity. And finally, the heat conducted from the molten droplets on the lower surface near the bottom of the cutting line was approximated with a uniform temperature distribution of 1527°C.
After the heat source modelling, the numerical simulation of heat conduction in a plate during the cutting process was done using FEM. The governing differential equation for heat conduction in a plate is as below:

$$\nabla \cdot (k\nabla T) - \rho c\frac{\partial T}{\partial t} + q = 0 \tag{2-17}$$

where T is the temperature, ρ is the density, c is the heat capacity, and q is the heat generation. In the simulation the material properties of the steel plate dependent on the temperature like specific heat and thermal conductivity were also incorporated. The heat source modelling was based on many data assumption like oxy-fuel efficiency to be 50% which is very low and also the heat flow model did not consider the phase changes in the cutting process.

Discussion: The findings of the study of various literature on numerical modelling of the heat source and temperature distribution was that the most of the analysis was done based on various assumption which is coherent for theoretical understanding of the process but not effective for the real world implementation. Also the metal in oxy-fuel cutting goes through the solid-gas-liquid phase change but none of the studies has taken this into account as it makes the model more complex. Also, the studies were done considering the infinite steel plate which is not going to be realistic for metal tubes as in our case.

Chapter 3

Research Questions, Aims & Objectives

3-1 Research Topic

The conclusion from the literature search in Chapter 2 is that temperature is the single most important parameter which could be used to monitor the cut quality. Thus this leads to the main research question based on what has been written in the Literature review and the company requirements is:

Is it possible to design a Dynamical Model of the Oxyfuel gas cutting process in order to be able to realize a control system which facilitates the automation of steel cutting?

Following this, below are the sub-questions that arise from the main research question:

1. How to identify heat transfer parameters which are important for the modelling of temperature distribution in the oxyfuel cutting process of steel?
2. How to investigate the flame conditions and the thermal effect of the heat supply Q(J) during the preheating process?
3. What are the factors affecting the heat transfer P(t) including the heat loss?
4. How to investigate the distribution of temperature in the metal sheet during the cutting process?

Here, we need to study the transfer of heat throughout the cut contour of the metal in the influence of oxy-fuel cutting conditions. The following modeling is required to study the effect.

1. Modeling of the temperature distribution over time along the cutting contour which involves the consideration of few dynamics like the effect of heat transfer based on the angle of the nozzle, the speed of cutting, the cutting contour and also the supply of fuel i.e heat input (oxy fuel).
2. Consideration of the feedback of the heat flow modelling with the heat input in order to be able to design a closed-loop system.
3. Modeling of the entire cutting material considering Periodic boundary conditions which are approximating a large (infinite) system by using finite space and time elements called *cells*.

3-2 Project Goals

- Determination of the dynamic model of the temperature distribution considering the process of melting/ phase change
- Comparison of the simulated results with the experimental results

Chapter 4

Methodology

The thermal model of oxy-fuel cutting is a complex mechanism as it includes analysis of features such as heat conduction, phase change, chemical reactions, coupled heat and mass transfer, and thermal stress analysis etc. It poses a series of key engineering problems. The complexity of practical problems is such that closed form solutions are not generally possible. The use of numerical techniques to solve such problems is therefore considered essential. Few amongst them are *Finite Element Method (FEM), Finite Difference Method (FDM), The Cell Method (CM)* etc. They are suitable for analyzing the steady and transient 1D/2D/3D heat flow during oxy-fuel cutting and they also use different thermal properties of materials to obtain result thoroughly. In the sections followed we are going to explain the two most efficient numerical methods to model the heat flow and temperature distributions. Section **4-1** explains the preliminaries of Finite Element Method (FEM) and the steps to model the heat conduction. Section **4-2** explains the Cell Method, an algebraic formulation approach and its implementation in order to formulate the physical phenomenon. Further discusses its advantages over the other numerical methods.

4-1 Finite Element Method (FEM):

It is a numerical method for solving physical problems, where the governing differential equations are available. The method essentially consists of assuming the piece-wise continuous function for the solution and obtaining the parameters of the functions in a manner that reduces the error in the solution. The main steps of how the FEM works is described below [28]:

1. *Discretizing the continuum:* Divide the solution region into non overlapping elements or sub-regions. The finite element discretization allows a variety of element shapes, for example, triangles or quadrilaterals. Each element is formed by the connection of a certain number of nodes.

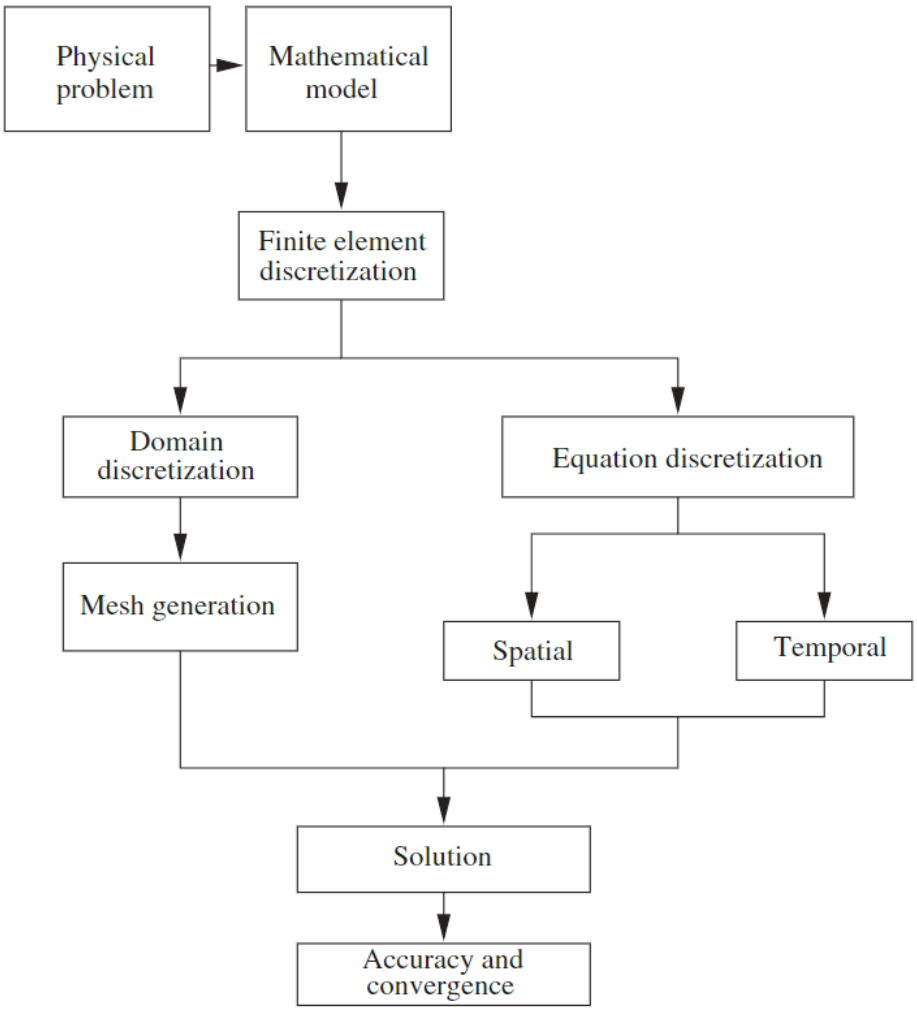

Figure 4-1: Numerical model for heat transfer calculations using FEM.

2. *Selection of interpolation functions:* The interpolation function represents the variation of the field variable over an element. The number of nodes to form an element, the nature and number of unknowns at each node decide the variation of a field variable within the element.

3. *Finding the element properties:* The matrix equation for the finite element should be established which relates the nodal values of the unknown function to other parameters.

4. *Assembling the element equations:* To find the properties of the overall system, we must assemble all the individual element equations. Boundary conditions should be imposed.

5. *Solving the global equation system:* The resulting set of algebraic equations may now be solved to obtain the nodal values of the field variable e.g temperature.

6. *Computing additional results:* From the nodal values of the field variables e.g temperatures, we can calculate the secondary quantities e.g heat fluxes.

Most of the literature studied in section 3.2.3, have done finite element analysis in order to analyse heat conduction in steel plate. As per Bae [11], the governing differential equation for heat conduction in a plate during the cutting process is given by equation 2-17. The governing finite element equation for heat transfer during flame heating can be expressed in matrix form as follows:

$$C(T)\dot{T} + K(T)T = Q \tag{4-1}$$

where $C(T)$ and $K(T)$ are the temperature-dependent heat capacity and the thermal conductivity matrix respectively, T is the nodal temperature vector, $\dot{T}$ is the time derivative of the temperature vector, and Q is the heat flux vector obtained via heat source modeling. The heat source modelling is explained in section 3.2.3. This heat source model is applied to solution domain figure 6-1. The initial nodal temperature of the domain is assumed to be ambient temperature. The heat flow through the model is then simulated using EEM, and the simulation is started when the heat source approaches the solution domain and lasted until the solution domain has cooled down to ambient temperature. Figure 4-3 shows the solution domain for a FEM numerical simulation, which is divided into 20,000 rectangular elements with four nodes per element.

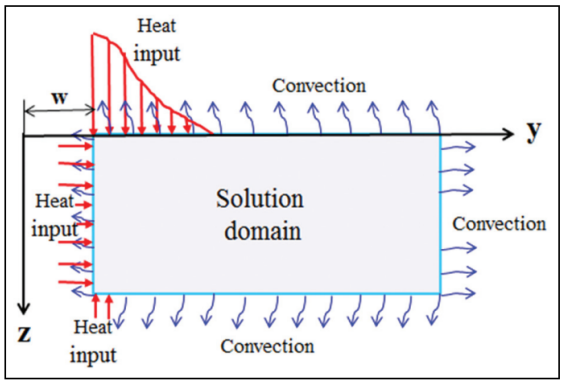

Figure 4-2: Solution domain with the boundary conditions for the thermal analysis [11].

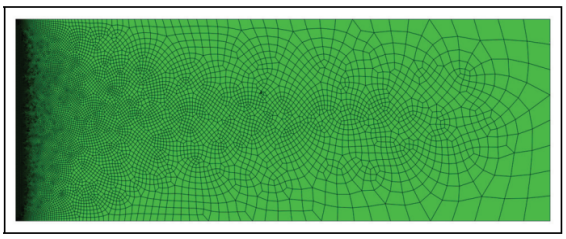

Figure 4-3: Division of the solution domain with finite element meshes [11].

The results of FEM analysis depends on mesh density of the model. Because, the coarseness of mesh can produce erroneous result, while too fine mesh size can increase the computational time [29].

4-2 The Cell Method (CM):

The classical numerical modelling approaches like (FEM, FV, FDM) relies on the discretization of Partial differential equations (PDE), whereas **The cell method (CM)** is an Algebraic Formulation (AF) approach which avoids entirely the discretization step by using algebraic formulation of physical laws starting directly from experimental measurements [1]. This formulation has the great merit of maintaining close contact between the mathematical description and the physical phenomenon described.

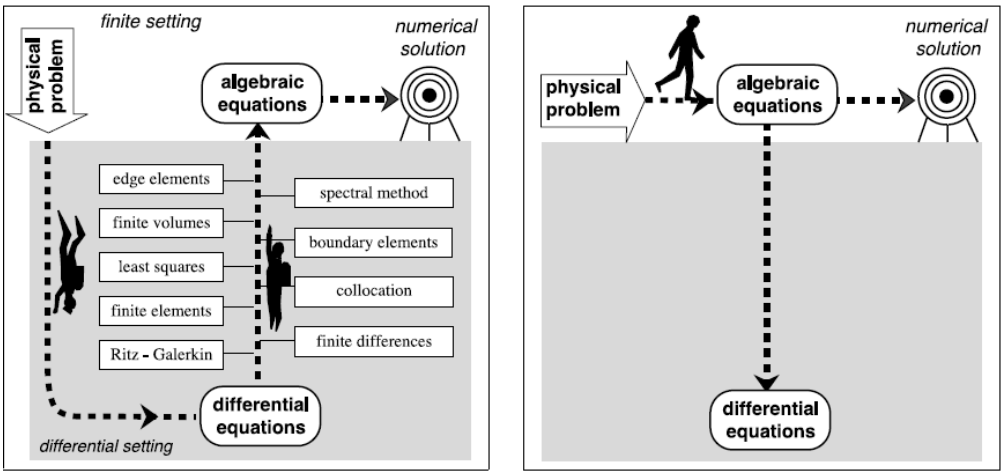

Figure 4-4: Path to obtain numerical solution to a physical problem using FEM (Left) and CM (Right) [12].

The AF makes use of *global variables*, that is, variables associated not to a point, like field variables in differential theories, but to a finitely-sized domain [30] i.e. finite sizes of spaces and finite intervals of time. These variables are neither densities nor rates of other variables. Specifically:

- a global variable in space is a variable that is not the line, surface or volume density of another variable;
- a global variable in time is a variable that is not the rate of another variable.

Based on the role of physical variables, global variables can be divided in three main categories:

- *configuration variable*, which defines the state of a system e.g temperature;
- *source variable*, which describes the factors responsible for the change in configuration e.g heat source, mass flow; and
- *energy variable*, which is obtained by the product of a configuration variable by a source variable e.g Gibbs free energy, enthalpy.

The equations used to relate the configuration variables of the same physical theory to each other and the source variables of the same physical theory to each other are known as *topological equations*, whereas those relating configuration to source variables, of the same physical theory, are *constitutive equations*.

These global variables are associated to a discrete space and time reference framework as mentioned above, called a *cell complex*. Now, since each physical phenomenon occurs in space, and space has a multi-dimensional geometrical structure, the global physical variables have a multi-dimensional geometrical content. As a consequence, all the global physical variables are associated with one of the four space elements, that is **P** (points), **L** (lines), **S** (surfaces), and **V** (volumes) which are the *p-cells* of the cell complex, with $p \in \{0, 1, 2, 3\}$ being the geometric dimension figure 4-5. Also the global variables in time are associated with the elements of a cell-complex, which has dimension 1 and generalizes the time axis. These two time elements **I** (time instants), **T** (time intervals) are represented by the nodes and lines of this one-dimensional cell-complex, respectively figure 4-7. These space and time elements are endowed with orientations which can be either an internal or an external orientation, in the latter case a tilde being used. The CM uses two cell-complexes: the primal cell-complex and the dual cell-complex, in relation of duality with the primal cell-complex figure 4-6. In particular, in 3-D space,

- each node of the dual complex is contained in one volume of the primal complex,
- each edge of the dual complex intersects a face of the primal complex,
- each face of the dual complex is intersected by one edge of the primal complex,
- each volume of the dual complex contains one node of the primal complex

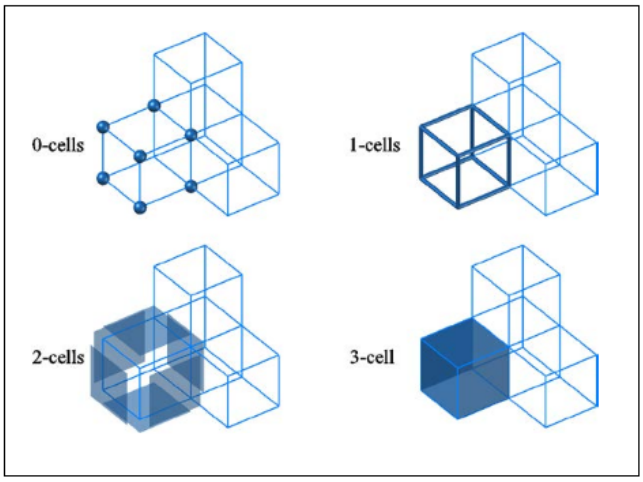

Figure 4-5: The four space elements in algebraic topology [13].

From a cell complex, which we shall call *primal* (inner orientation), by considering a point inside each 3-cell, say its barycenter, one can construct another cell complex, called *dual* (outer orientation), by taking these points as vertices of dual complex figure 4-8.

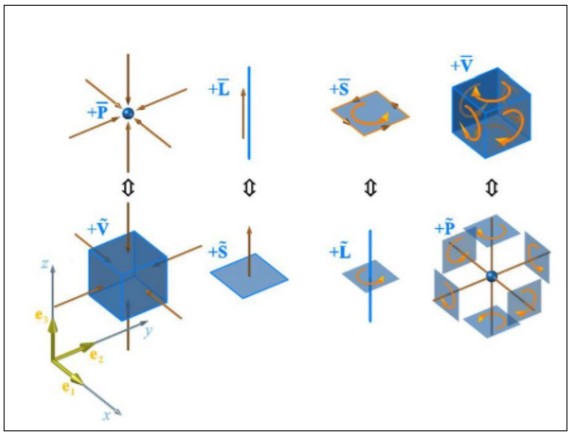

Figure 4-6: Relationship between the inner orientation of a p-space element and its dual element, of dimension $(p-1)$ [14].

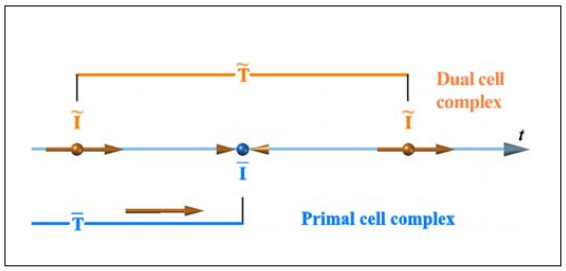

Figure 4-7: Time elements and their duals with orientations [14].

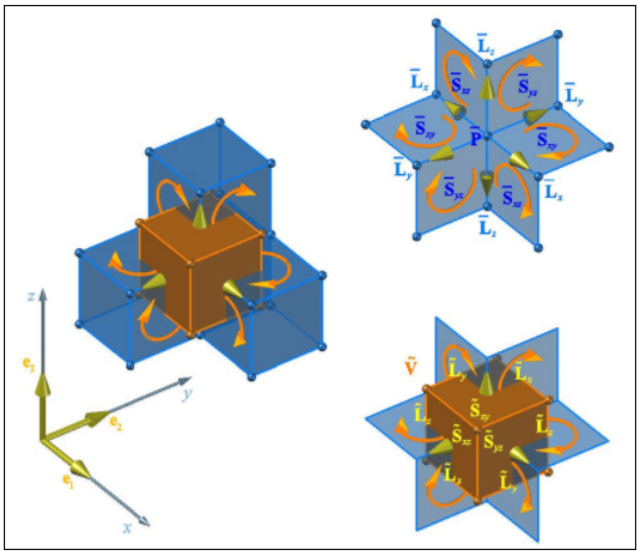

Figure 4-8: Relation of duality in three-dimensional space, between inner orientations of the primal cells and outer orientations of the dual cells [15].

To make the understanding of link between global variables and space elements of a cell complex clear, lets examine it in the case of thermal field. In figure 4-9, Internal energy and heat source are global variables which are associated with the 3-cells of the dual complex; heat fluxes are associated with the 2-cells of the same complex. The temperature of each 3-cell is the one measured in some "central" point of the cell, say its barycenter, i.e. a 0-cell of the primal complex. The temperature difference refers to the line connecting two barycenters, i.e. to a 1-cell of primal complex. Doing so, we see that the configuration variables, i.e. temperature and temperature difference, refer to the elements of the primal complex, while the source variables, i.e. internal energy, heat source and heat flux, refer to the elements of the dual complex.

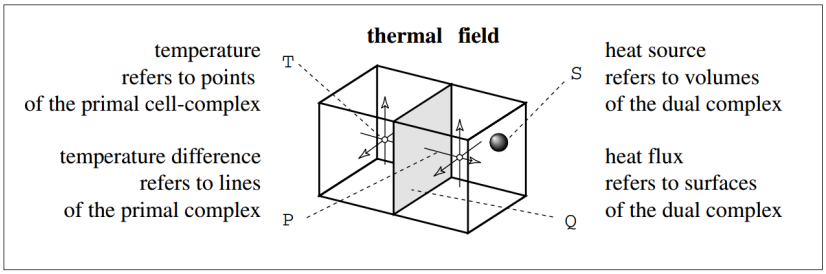

Figure 4-9: Physical variables and cell complexes

Summary of the features of CM:

- It works on unstructured grids.
- it works even in presence of different materials.
- it gives rise to a diagonal mass matrix, hence it produces an explicit time stepping scheme;
- it avoids the integration on lines, surfaces and volumes because it makes use directly of global variables;
- it uses two cell complexes in space and in time, one dual of the other. Some variables are evaluated at the primal instants, while other at the dual instants: this choice is not arbitrary but stems from the physical meaning of the variable. This avoids loss of accuracy, instability and the violation of energy conservation;
- physical equations are directly written in algebraic form, without the intermediation of the differential formulation and can be directly implemented; the displacement field within each primal cell is considered as affine and higher degree interpolations are possible; the other is that the velocity of the center of mass of the dual cell is approximated to the velocity of the corresponding primal node [31];
- the core of the direct algebraic formulation are the dual cells;
- the boundary conditions involving forces are included the fundamental equation;
- is valid also for a non linear constitutive equation;
- the direct algebraic formulation is automatically consistent. In fact, it performs the same steps that lead to the differential formulation, but operating on a finite portion (dual cell) rather than an infinitesimal portion of the continuum.

Advantages of CM:

The advantages of Algebraic formulation approach employed in the Cell Method is discussed below:

- The truly algebraic formulation provides us with a numerical analysis that is more adherent to the physical nature of the phenomenon under consideration. Hence it leads to the structure preservation and strict enforcement of the conservation laws. Moreover, the algebraic formulation preserves the length and time scales of the global physical variables since it avoids the limit process.
- Providing an algebraic system of physical laws is a mathematical expedient, needed in computational physics because computers can only use a finite number of algebraic operators.
- The CM offers an interdisciplinary approach, which can be applied to the various branches of classical and relativistic physics.
- Finally, differently from their variations, the global variables are always continuous through the interface of two different media and in presence of discontinuities of the domain or the sources of the problem. Therefore, the CM can be usefully employed in problems with domains made of several materials, geometrical discontinuities (corners and cracks), and concentrated sources.

Chapter 5

Experimentation

5-1 Introduction

The experiments were performed in order to validate the developed numerical models. The various sets of experiments were carried out in the workshop of HGG, Wieringerwerf. To verify the numerical simulation, a series of cutting experiments were performed in accordance with the combinations of the cutting parameters used for the simulation. The experiments were based on the working principle of oxy-acetylene cutting which is, once the work-piece is brought to the ignition temperature by providing heat energy generated by the combustion of oxygen and acetylene, the pure oxygen under high pressure is supplied which oxidizes the work-piece. Also, the high-pressurized oxygen supply blows the liquid metal out of the kerf. This generated combustion heat which in turn heats the underlying layer to the ignition temperature and the process continues autogenously and cuts the metal.

5-2 Experimental Set up

A view of the experimental set-up is shown in figure 5-1. It consisted of:

1. **SPC 3000 (Stationary Pipe Cutting Machine):** SPC is a very robust machine built to handle large pipe diameters ranging from $75mm$ to $3000mm$ and heavy weights till $60t$. We used SPC to cut the metal sheets. It is suitable for Plasma as well as Oxy-fuel cutting. It is equipped with a patented biaxial cutting head to perform 3D cutting which consists of a burner and a nozzle for the outlet of oxygen and acetylene gas. It has an integrated connections between the machine and the CAD packages to provide the design of cut. It has a touch screen interface which is clear, intuitive and easy to operate.

2. **Thermal camera:** A high resolution radiometric infrared thermal imaging camera FLIR T640, was used for performing experiments. It involves measurement of infrared

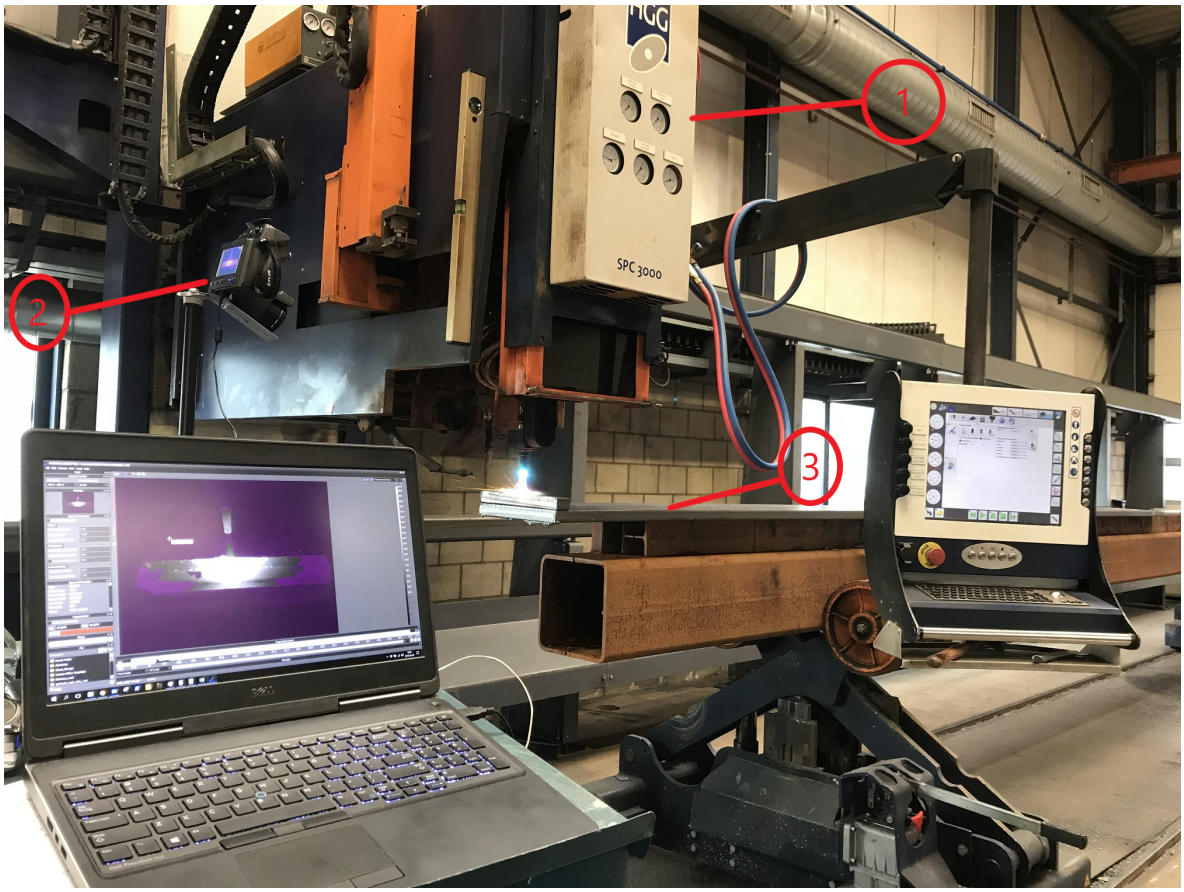

Figure 5-1: Experimental set-up

wavelengths of spectral range (7.8 - 14μm) to determine temperatures during the cutting process by using infrared sensitive photographic film. The temperature range selected for this investigation was $-20°C$ - $1500°C$ with thermal sensitivity as low as $0.045°C$. The thermal imagers are fully radiometric which means they measure and store temperatures at every point in the image. While the arrangement of pixels describes the spatial structure of an image, the radiometric characteristics describe the actual information content in an image. Main advantages of thermal camera is the fast response, no adverse effects on measured temperatures, no physical contact, and allowing measurements on objects which are difficult to access.

3. **Metal sheets:** The steel plate used for cutting was S235JR variant of structural steel of 30mm and 50mm in thickness. Structural steel grades are designed with specific chemical compositions and mechanical properties formulated for particular applications. The chemical composition of the steel used is stated in the table 5-1.

Carbon	0.17% max
Manganese	1.40% max
Phosphorus	0.035% max
Sulfur	0.035% max
Silicon	0.035% max

Table 5-1: Chemical composition of the steel used (S235JR)

4. **Thermocouples:** Thermocouples are one of the most widely used experimental methods for measuring the temperature in machining. Thermocouples are conductive, inexpensive, can be operated over a wide temperature range and can be easily applied. However, they only measure the mean temperature over the entire contact area of the tool and the work piece. The K-type thermocouple was used for the measurement of temperature in the experimentation. It is capable of measuring temperature ranging from -200 to 1250 degree Celsius. The thermocouple measures temperature and generates corresponding emf which is measured by the multimeter. The output obtained from the thermocouple circuit is calibrated directly against the unknown temperature. Thus the voltage output obtained from thermocouple circuit gives the value of unknown temperature directly.

5-3 Description of the experiments

The oxy-acetylene flame was used to cut the steel plate with varying thickness at varying speeds using the gas containing oxygen and acetylene with the flow rates and pressure as prescribed by the HGG standard cutting chart. The temperatures along and around the cutting direction were measured by the thermal camera configured. The HGG standard cutting chart parameters were used as a reference to establish the settings for the various types and sizes of nozzle tips for different thickness of the metal. The temperature distribution is dependent on various factors like preheat gas pressures, since the gas flow pressure is directly proportional to the velocity of the gases, and transfer of heat from flame to metal is partly dependent on the impingement of the hot gas molecules on the surface of the metal plate. The type and size of tip also influence heat transfer, since they contribute to gas flow. But we assumed all these aforementioned factors to be constant for all the cuts to simplify the process. The pressure at which the gas were supplied is mentioned in the table 5-2.

Preheat gas	0.16 bar
Preheat Oxygen	0.79 bar
Gas	0.11 bar
Oxygen	0.2 bar
Cutting Oxygen	5 bar

Table 5-2: The supply pressure for the gases used in preheating and cutting

Quantitative thermal imaging requires that a true temperature value be assigned to each pixel

in the image, and is subject to problems unique to infrared thermography. Key issues include,

- Reflections from surrounding objects. Most metals, reflect thermal radiation much like a mirror reflects visible light. Reflections can lead to misinterpretation of the thermal image. The reflection of thermal radiation from the operator's own body might lead to a false temperature reading. In order to minimize such reflections, the angle at which the thermal imaging camera was pointed at the object was chosen carefully [32].
- Knowledge of surface emissivity. Emissivity (ϵ) is a material property, and is defined as the ratio of the radiation from a body to the radiation of a black body at the same temperature. It is common to determine emissivity using the temperature of the object determined by the thermal radiation method, together with an absolute temperature measurement of the object - such as by thermocouple.

5-3-1 Calculation of Emissivity

There are two basic approaches to determining surface emissivity; surface treatment or material heating. Surface treatment involves applying a treatment that is of a known high emissivity (usually tape or paint) to the surface of the object and then heating the surface. Material heating involves uniformly heating the object to a known steady-state temperature that is above ambient temperature [33]. Since surface treatment of the steel plates were not feasible, the material heating method was employed to determine the emissivity of the material.

Below steps were followed to determine steel plate's emissivity using the material heating method.

1. Heated the object to a known uniform steady-state temperature which is $1200K$ by providing heat from the oxy-acetylene flame.
2. Measured the steady-state temperature of the object by using a contact temperature probe i.e thermocouple.
3. Adjusted the emissivity of the thermal camera until the temperatures recorded by the camera are equal to the temperatures of the steel plate measured in step 2.

The emissivity recorded for the steel plate was *0.95*.

5-3-2 Cutting metal by varying speed

It has been established from the study of the literature that temperature is the is the single most important parameter which could be used to monitor the cut quality. And the distribution of temperature is greatly influenced by the variations in the cutting speed. In order to verify this, the cutting speeds were varied to produce poor quality cuts. The criteria used to determine or grade the quality of cuts included (as shown in figure 5-2):

1. Smooth finished plate surfaces without any drag lines.

Figure 5-2: The cut having smooth plate surface with clean sharp edges free from slag

2. Clean and square edges free of slag deposits.

The cut in figure 5-2 was obtained on the $30mm$ thick plate by moving the nozzle at the speed of $450mm/min$ as prescribed by the [34]. When the cutting speed is normal, there is sufficient oxygen for the oxidation process and temperature distribution to happen. This leads to metal being evenly heated thereby leading to good quality straight cuts. The 2-D plot in figure 5-4 shows the temperature distribution during the cut shown in figure 5-3. The maximum temperature that is reached after the cut is $1239.35K$.

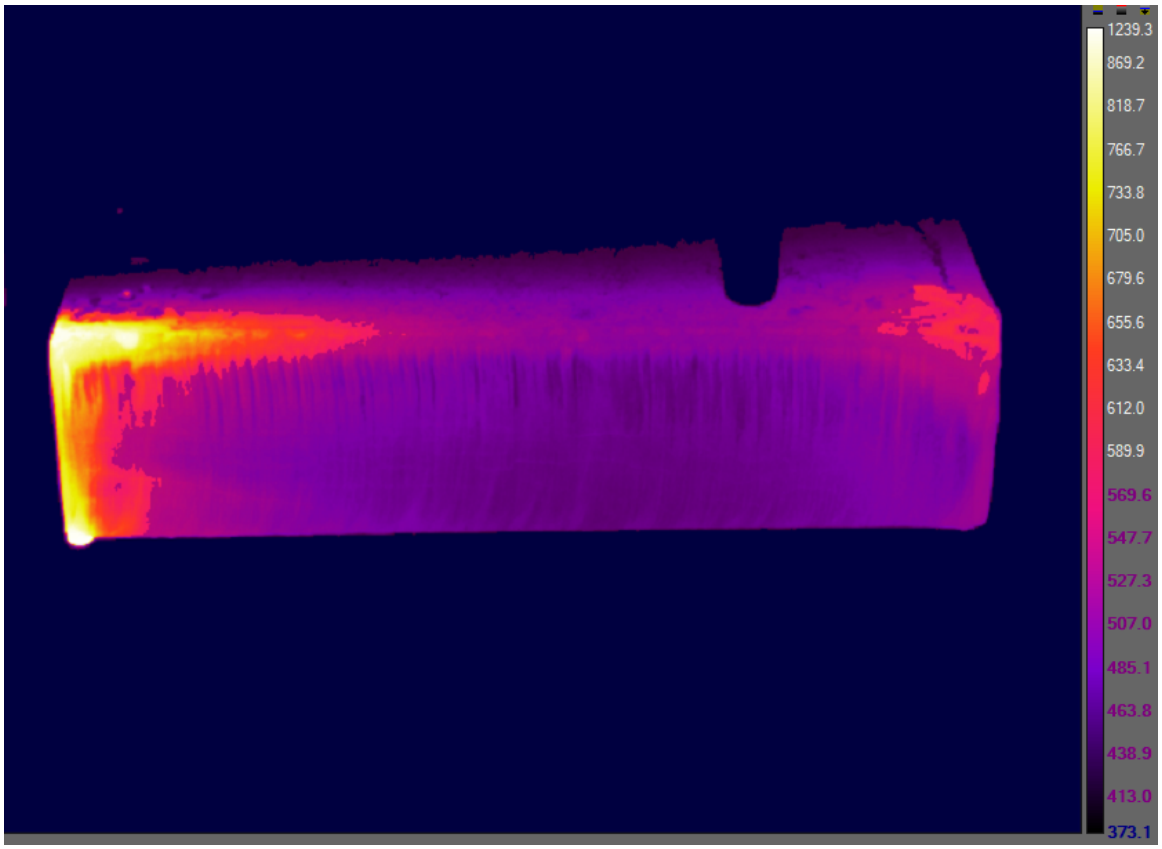

Figure 5-3: The cut with the temperature distribution

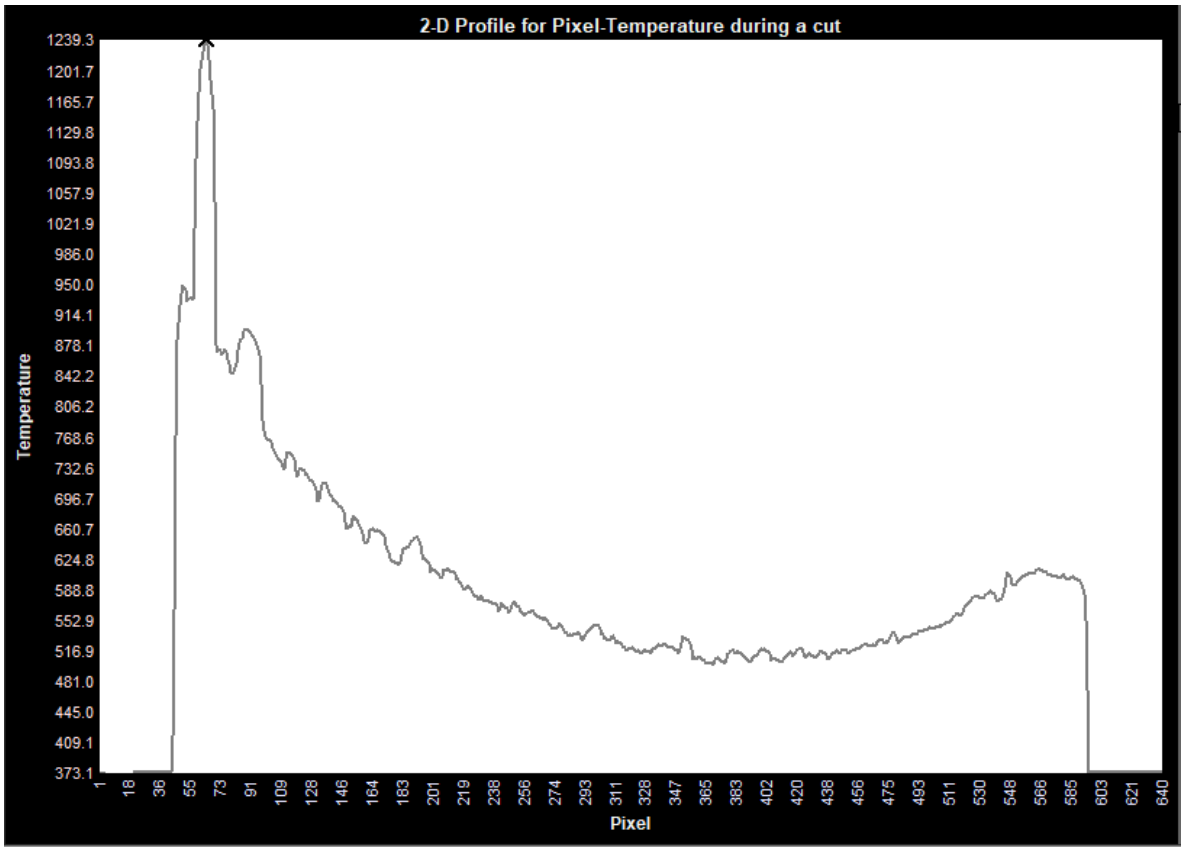

Figure 5-4: Temp v/s pixel plot at the end of the metal cut

The figure in 5-5 shows the process of metal being cut and the temperature distribution followed in it. The white border in the picture depicts the line of cut which starts from the position marked 1. At position 1 the preheating takes place and the temperature of the metal piece is brought to the ignition temperature. Once the metal piece is ignited, the further oxygen supplied is utilized in the oxidation reaction which is highly exothermic and hence producing sufficient heat required for the cutting of the metal piece. The heat is propagated evenly and we obtain the uniform temperature distribution in the metal piece. A thermal steady state is reached and temperature histories are transformed into temperature profiles in a frame attached to the torch using the cutting speed. These profiles are used later to calibrate the missing input parameters of the heat flow model.

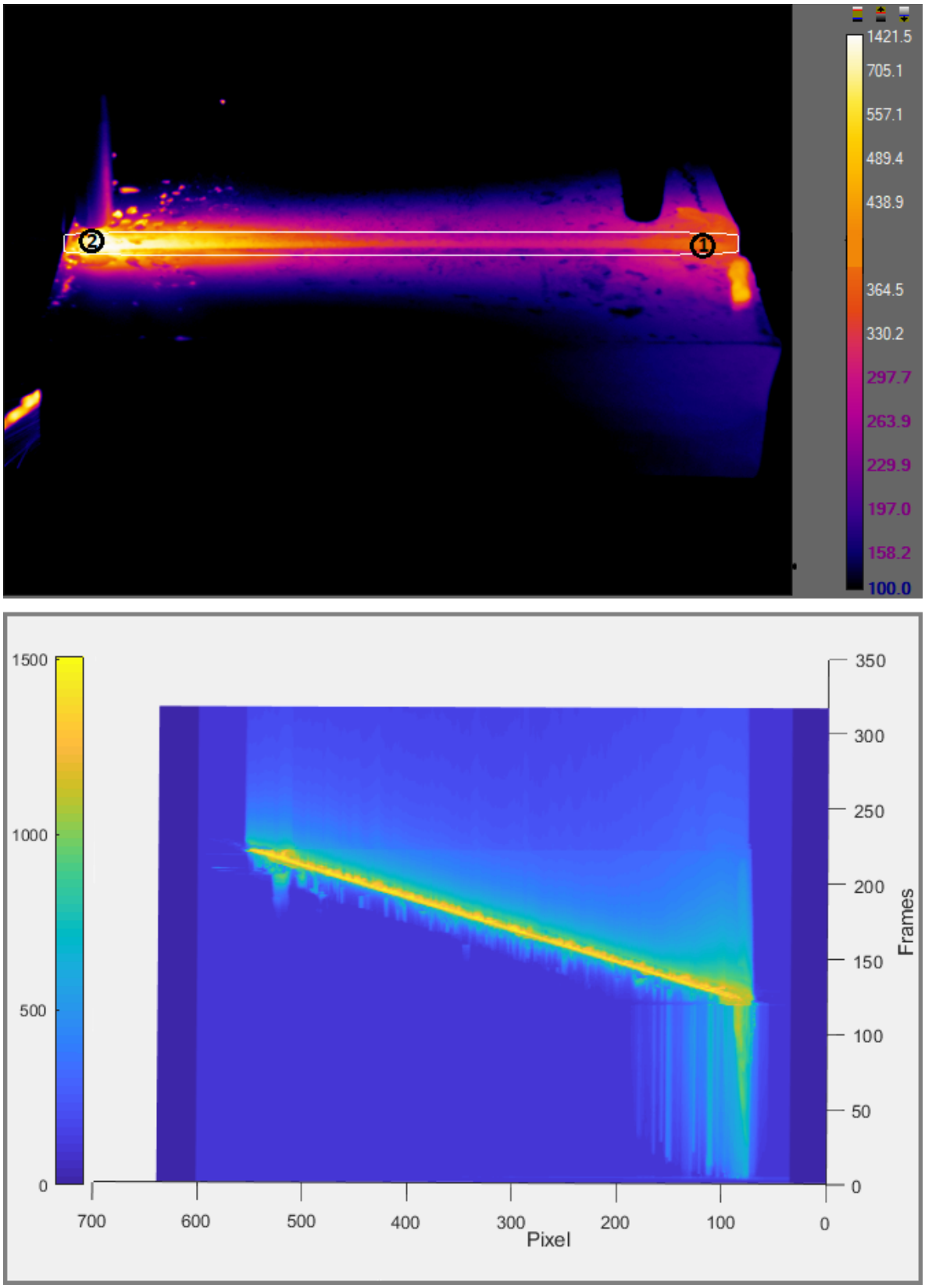

Figure 5-5: Temperature distribution in the metal in the process of cut

Inferences:

Below are the few inferences drawn after performing experiments on the cutting of steel by varying the speed.

1. Higher cutting speed, lowers preheat and the quality of the cut goes down. Top edge remains relatively clean and square while the bottom of the cut has excessive slag due to incomplete oxidation. There are pronounced drag lines slanting away from the direction of the cut as shown in figure 5-6.
2. If the cutting speed is too low, availability of excessive oxygen combined with excessive preheat could cause gouging. This results in an uneven temperature distribution in the kerf. The edges are rough and uneven as shown in 5-7.

All these degradations in cut quality are related to excessive temperature of the plate and, in the case of gouging, to excess supply of cutting oxygen available for oxidation, which is further dependent on the temperature distribution.

Figure 5-6: Cutting metal at higher speed

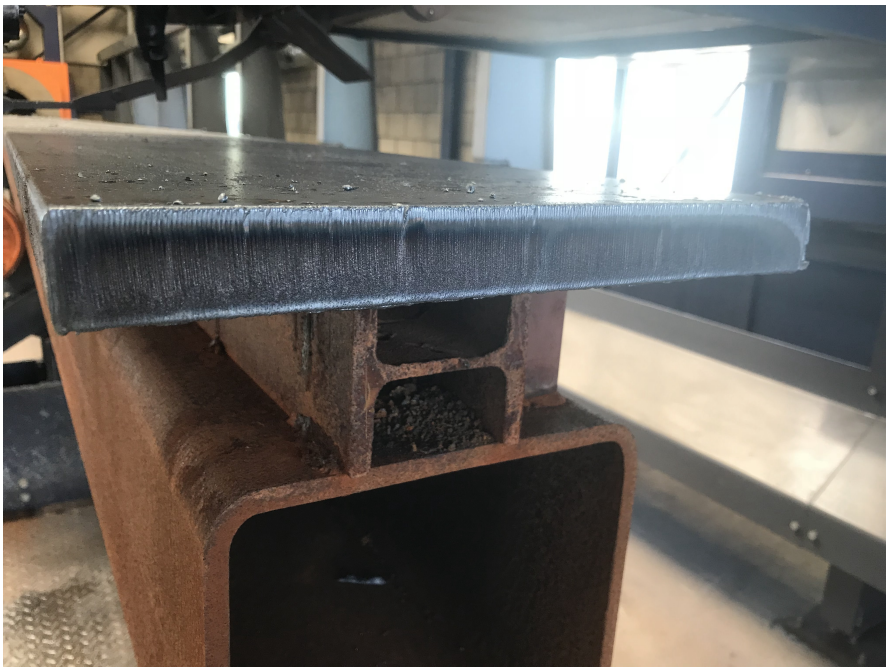

Figure 5-7: Cutting metal at slow speed

5-3-3 Cutting metals with varying thickness

For this set of experiments, metal piece of 50mm thickness was used. The thicker plates require more heat input to bring it to the ignition temperature hence as per [34], the different set of cutting and preheating nozzles were used compared to the one used for the metal with 30 mm thickness. Also, for the thicker materials slower cutting speed is used. Hence for this fact, for thicker materials lower preheat flame input was required while cutting because of slower cutting speed. The 2-D profile plot for the same is shown in figure 5-8.

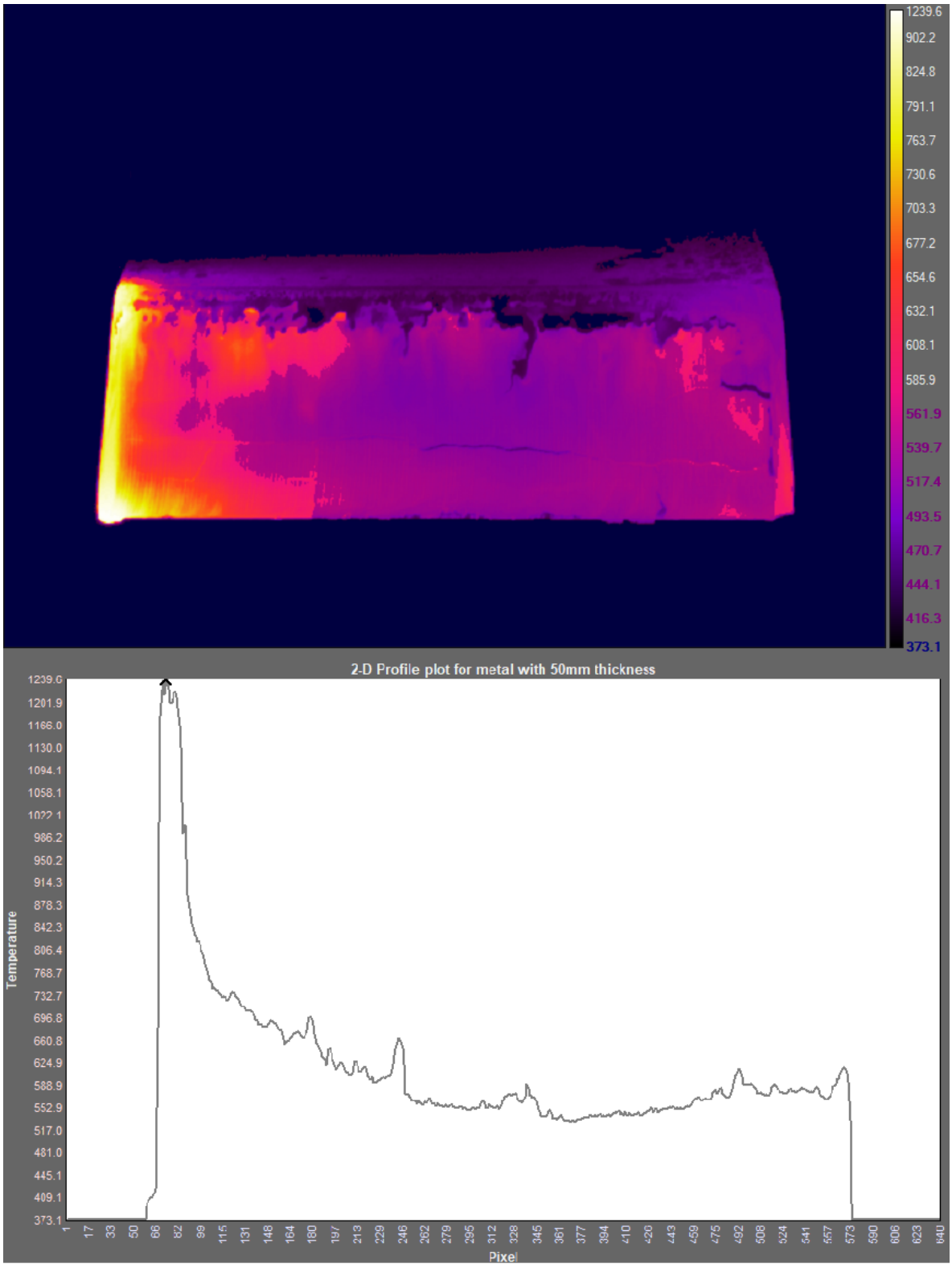

Figure 5-8: Cut and the Profile plot of the metal with 50 mm thickness

Discussion:

1. After comparing the profile plot of the cut for metal with varying thickness, it can be established that although the heat input requirements for different thicknesses of material are different, but the cutting process maintains a maximum temperature of $1200 - 1300K$.

2. The analytical work also shows that approximately 66 percent of the energy for preheating is provided by preheating flame and 34 percent by the exothermic chemical reaction. And that is why there is a bump at the starting point.

The figure 5-9 shows the cut obtained by placing two metal piece on top of each other. This was done to increase the thickness of the metal to 60mm. The cutting speed was chosen to be 250mm/ min as prescribed for the metal with thickness 60mm. The top metal sheet got cut with nice cut quality but the bottom metal piece had gouging and the slag deposited. The explanation of this would be the presence of air between the two metal piece. Air is established to be the very poor conductor of heat and hence most of the heat was lost before reaching the bottom metal piece. This led to the uneven temperature distribution thereby producing uneven cut with gouges.

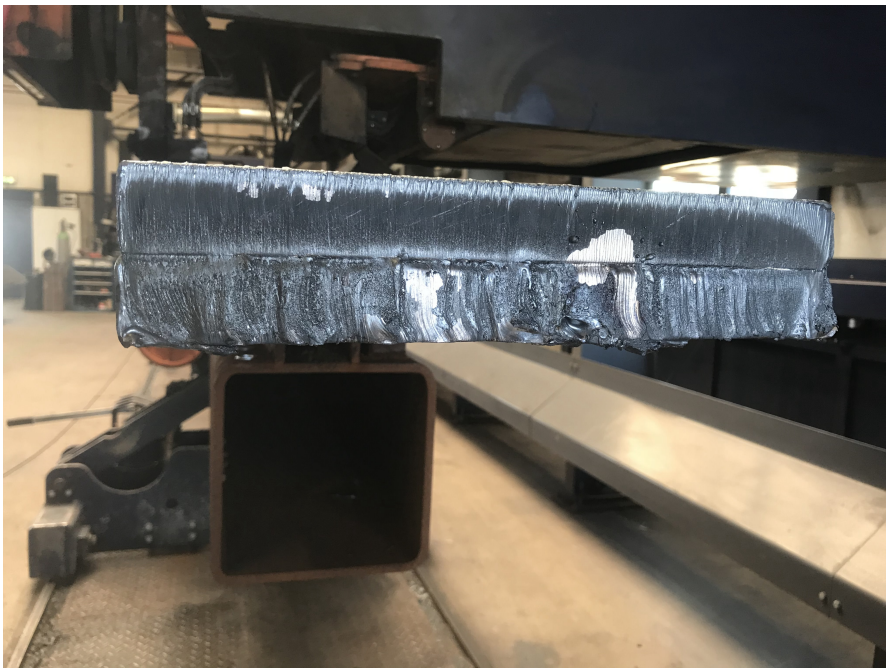

Figure 5-9: Cut with gouges due to air between two metal pieces

Chapter 6

Numerical Modelling

6-1 Transient thermal conduction in solids using CM

In case of standard PDE approach, the formulation of the transient thermal problem is based on the conservation of energy i.e. the energy variation in a volume over a period of time is equal to the difference between the heat produced and the out flowing heat [35]. The partial differential equation is given by

$$\rho c \frac{\partial T}{\partial t} - \nabla . \lambda \nabla T = \sigma \tag{6-1}$$

where, ρ is Mass density, c is Specific heat, T is Absolute temperature and σ is the Heat source. This equation is usually discretized using a FEM [12].

In the contrary the CM is based on the construction of the Tonti diagram for the physical phenomenon and its direct translation into a numerical method (figure 6-1). Here,

- Configuration variables:
  - Temperature (T_h) is the thermodynamic temperature (in Kelvin) at the point p_h and time instant I. It is associated with the point. Since it defines the state of the system, it is a configuration variable and hence associated with the primal cell (inner orientation). Hence it is written as, $T_h[\bar{I}, \bar{P}]$.
  - Temperature gradient (G_α) is the relative temperature (in Kelvin) associated with the line l_α and time instant I i.e change in temperature as a function of distance. It is associated with the line. Since it also defines the state of the system, it is a configuration variable and hence associated with the primal cell (inner orientation). Hence it is written as, $G_\alpha[\bar{I}, \bar{L}]$.
- Source variables:

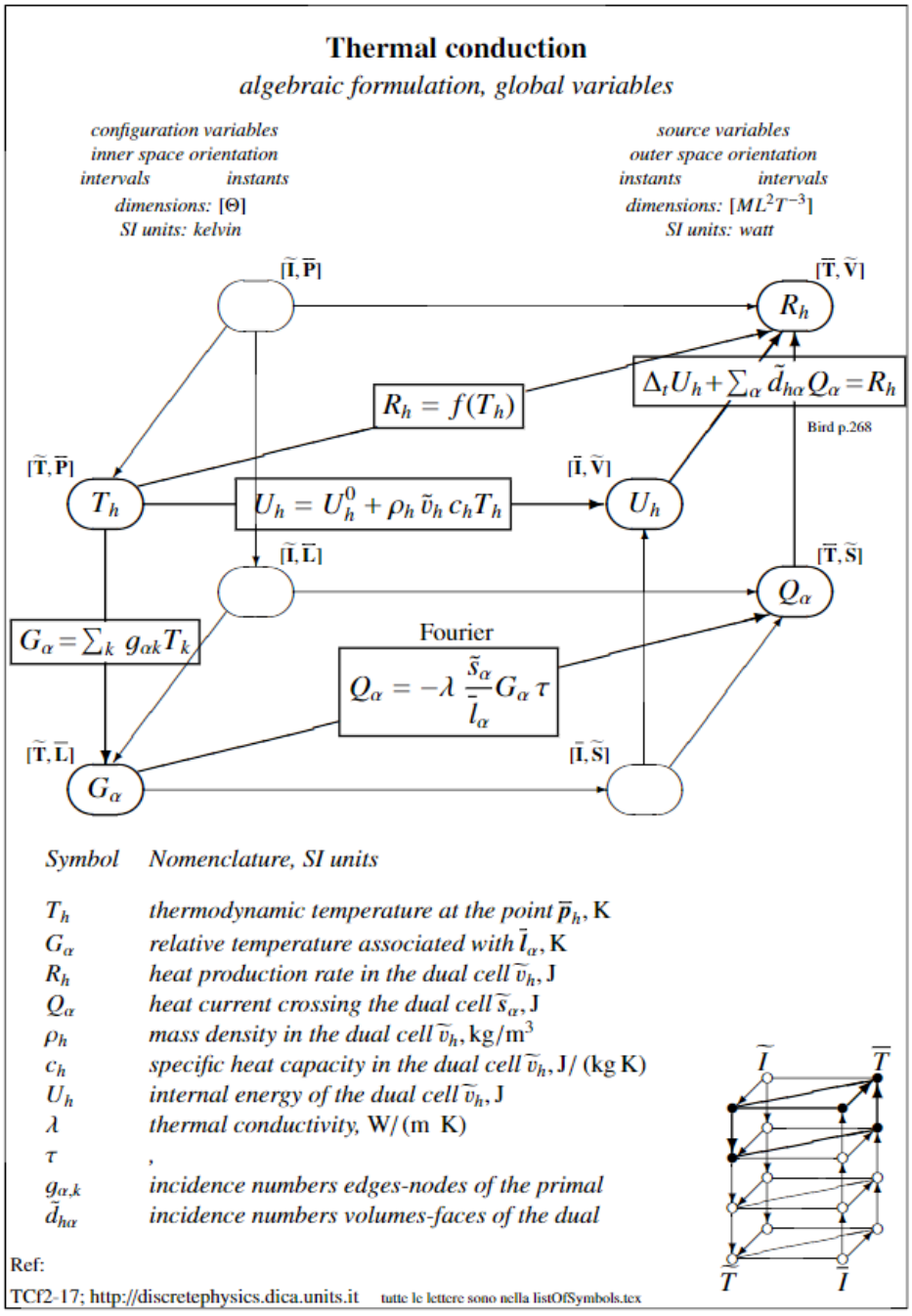

Figure 6-1: Thermal conduction in solids based on CM [1]

– Heat current crossing through the surface of the dual cell is (Q_α) in Joule and since it describes the factors responsible for the change in the configuration of the system, it is a source variable with outer orientation. Hence it is written as, $Q_\alpha[\bar{T}, \tilde{S}]$.

– R_h is the heat production rate in the dual cell in Joule. It is also the source variable associated with the volume of the dual cell. Hence it is written as, $R_h[\bar{T}, \tilde{V}]$.

- Energy variables:
  - Internal energy (U_h) of the dual cell in Joule is the energy variable associated with the volume of the dual cell. It is written as, $U_h[\bar{I}, \tilde{V}]$.

After defining the variable, we need to establish the balance and constitutive equations which relates the configuration variables and source variables to each other and configuration to source variables respectively.

- Balance Equations: The relation between the defined Configuration variables to each other and the defined Source variables to each other.
  - The relation between T_h and G_α:

    $$G_\alpha = \sum_k g_{\alpha k} T_k$$

    Here, $g_{\alpha k}$ is the incidence numbers edges-nodes of the associated primal cells
  - The relation between Q_α, R_h and U_h is the rate of change of the internal energy plus the summation of heat currents flowing through the all the associated surfaces of the dual cell, i.e :

    $$R_h = \Delta_t U_h + \sum_\alpha \tilde{d}_{h\alpha} Q_\alpha$$

    where, $\tilde{d}_{h\alpha}$ is the incidence numbers volumes-faces of the corresponding dual cell
- Constitutive Equations: The relation between the defined Configuration and Source variables.
  - The relation between G_α and Q_α. The Fourier law defines the relation between the two

    $$Q_\alpha = -\lambda G_\alpha \frac{\tilde{s_\alpha}}{\bar{l_\alpha}}$$
  - The relation between U_h and T_h. From the First Law of Thermodynamics we can state the relation between the two as:

    $$U_h = U_h^0 + \rho_h \tilde{v}_h c_h T_h$$

    where, ρ_h is the mass density associated with the volume of the corresponding dual cell (kg/m^3),
    $\tilde{v}_h$ is the volume of the corresponding dual cell and
    c_h is the specific heat capacity the volume of the corresponding dual cell ($J/(kgK)$).

Once the equations are established, we need to define the boundary conditions and configuration, source and the energy variable and computed and updated for the next cell.

The basic anatomy of main tasks required by the CM for the numerical simulation is provided below [36].

Anatomy of simulation code:

1. *describing the geometry and generating the mesh:* Based on 2D/3D modelling, the mesh is created as triangles or quadrilaterals in 2D and tetrahedron or hexahedron in 3D.
2. *building auxiliary data structures:* All the data concerning the geometric data structure mesh are stored in data structure, in order to make the input/output of the subsequent functions easy.
3. *building the gradient matrix:* This consists of the temperature behaviour inside the mesh and is expressed in terms of the nodal values.
4. *building a data structure for the material properties:* This considers the data pertaining to the material properties (like thermal conductivity) and heat source which is utilized in the formation of constitutive matrix.
5. *building the constitutive matrix:* The constitutive matrix for thermal problems links the primal edges to the dual faces i.e. the source variable with configuration variable. This constitutes the material properties and heat source. The constitutive equations governing the heat conduction are shown in figure 6-1.
6. *setting the boundary conditions:* The boundary condition can be the assigned temperature, the imposed thermal flux, thermal convection and thermal radiation. These conditions are imposed on boundary nodes (the nodes which belong to the boundary faces). The boundary faces can be identified because they are only referenced by one tetrahedron(in case of 3D).
7. *assembling the final system and finding the solution:* In this final step the matrices are arranged in order to find the unknown variables.

6-1-1 Anatomy and Pseudo-code of Heat conduction in 1-D using the CM:

The objective of the code is to solve a 1D transient heat conduction problem using the Cell Method. The three main phases of each numerical code dealing with the heat conduction process are:

- *Pre-processing*: builds the data structures, defines the material properties, initial and boundary conditions, assembles the stiffness and gradient matrices;
- *Computation*: at every time step, imposes the boundary conditions and solves the final system in order to compute the temperature in the next time step;
- *Post-processing*: calculates the derived quantities and plots the solution (scalar and vector quantities).

Assumptions: Material is considered isotropic i.e it's properties are constant across different spatial directions, here (x-axis). In other words: *density (ρ)*, *thermal conductivity (λ)*, *specific heat capacity (c)* are constant for the entire metal rod. These properties are also time and temperature independent.

Anatomy of pre-processing:

1. The first step is to describe the geometry of the rod. It consists of defining the *length (l)* and the *area of cross-section(A)* of the rod.
2. Define the time step Δt
3. Then we need to build a data structure for the material properties; i.e defining ρ, λ, c.
4. Next is the building of the auxiliary data structures for the primal and dual mesh.
5. Calculate *Mass* (M) matrix as $\tilde{v} \times \rho$ where $\tilde{v}$ is *dual volume*
6. Then is the building of the gradient matrix (G) which is the relation of *edge-to-node*.
7. Next is the defining of the input heat distribution source (Q). Source terms are associated to the dual structure, and in particular to dual volumes ($\tilde{v}$).
8. Then the last step in this section is to define the *Initial and Boundary Conditions*. The Robin boundary condition is used to simulate the behaviour of heat conduction in a rod whose one end is at a constant temperature (a Dirichlet boundary condition) but the other end exposed to the atmosphere, where heat loss occurs to the surroundings.

Pseudo-code of pre-processing:

Algorithm 1 Pre-processing

1: **procedure** STEPS FOR PRE-PROCESSING
2: Define $l, A, \Delta t$ *length in m and area of cross-section in* m^2
3: Define ρ, λ, c *Thermodynamic Temperature in K attime*(k)
4: Define $\bar{p}, \bar{l}, \bar{s}, \bar{v}, \tilde{p}, \tilde{l}, \tilde{s}, \tilde{v}$ *Data structure for primal and dual mesh*
5: Compute $M = \tilde{v} \times \rho$ *Mass matrix*
6: Compute G *Gradient matrix*
7: Define Q *Input heat distribution source*
8: Define T_0, S_B *Initial and boundary conditions*

Anatomy of Computation:

1. Set the *initial time (k)* and initialize *Thermodynamic temperature (T_k)* and *Internal energy (U_k)* of the rod at the time k in Kelvin and joule respectively.

2. Compute *Relative temperature (R_K)* at the time instant k by multiplying Gradient matrix with the Thermodynamic temperature i.e $G \times T_k$.

3. Then the *Heat current (S_k)* is computed at the time instant k using the Fourier's law for heat conduction.

4. Next is the calculation of the *Total heat production rate ($S_{total,k}$)* at time instant k, which is the sum of S_k, S_B and S_{ext} where,
   S_B is the heat current at the boundary with the loss of heat due to other end of rod being exposed to the atmosphere which is, $S_B = h \times A \times T_k - T_a$. Here, h is convective heat transfer co-efficient and T_a is the atmospheric temperature.
   S_{ext} is the external heat supplied due to the chemical reactions.

5. Then is the calculation of the *Heat balance (U_{k+1})* which is the summation of the U_k and $S_{total,k}$.

6. Next is the calculation of temperature at next time step i.e T_{k+1}.

7. The final step is to update the time step and repeat the steps from 2 till 7 until the end of simulation .

Pseudo-code of Computation:

Algorithm 2 Computation

1:	**procedure** STEPS FOR COMPUTATION	
2:	Set k	*Initial time in seconds*
3:	Initialize T_k	*Thermodynamic Temperature in K attime*(k)
4:	Initialize U_k	*Internal energy in joule attime*(k)
5:	***top***:	
6:	Compute $R_k = G * T_k$	*Relative temperature in K*
7:	Compute $S_k = -R_k * \lambda * \frac{A}{l} * \Delta t$	*Heat current in joule*
8:	Compute $S_{total,k} = S_k + S_B + S_{ext}$	*Heat production rate in joule*
9:	Compute $U_{k+1} = U_k + S_{total,k}$	*Heat balance in joule at time (k+1)*
10:	Compute $T_{k+1} = \frac{U_{k+1}}{c \times M}$	*Temperature in K at time (k+1)*
11:	Update $k = k+1$	*Next time step in seconds*
12:	**goto *top***	

6-1-2 Anatomy and Pseudo-code of phase change due to melting in 1-D rod using the CM:

Anatomy of pre-processing:

1. Define the *specific latent heat of melting (Q_m)* of steel rod.
2. Define the initial condition i.e the solid mass content in dual volume M_k. There is no boundary condition as the melting process is traversal.

Pseudo-code of pre-processing:

Algorithm 3 Pre-processing

1:	**procedure** STEPS FOR PRE-PROCESSING	
2:	Define Q_m	*Specific latent heat of melting of steel*
3:	Define M_k	*solid mass content at time k*

Anatomy of Computation:

1. Compute *heat available for melting (Q_{ext})* in joule. It is the difference between the total input heat and the heat conducted to the neighbouring cell.
2. Then check if the *Temperature (T_k)* at the time instant k is less than the *Melting temperature* T_m of steel, then run the algorithm for the heat transfer due to conduction else equate T_k and T_m. And update the new mass at the next time instant
$$M_{k+1} = M_k - \frac{Q_{ext}}{Q_m}$$
3. Now, check the updated mass M_{k+1}. If it is less than or equal to zero update it to 0 as the mass can not be negative. Ans remove the cells with zero mass from the cell complex.
4. Update the Internal energy as per the mass melted away.

Pseudo-code of Computation:

Algorithm 4 Computation

procedure STEPS FOR COMPUTATION
  Compute $Q_{ext} = Q_{total,k} - Q_c$ *Heat available for melting in Joule*
  if $T_k \geq T_m$ **then**
    $T_k = T_m$
    $M_{k+1} = M_k - \frac{Q_{ext}}{Q_m}$
  else
    Run algorithm 2
  if $M_{k+1} < 0$ **then**
    $M_{k+1} = 0$
  Remove cell with the zero mass
  Update $U_{k+1} = U_k \times \frac{M_{k+1}}{M_k}$

6-2 Discussion and Results

The proposed heat source models were applied to the solution domain. The simulation was done for the heat conduction and phase change. The heat input provided by the preheating and cutting flame as well as the chemical reaction was considered based on the data obtained by performing experiments. The corresponding modelling was not performed for the same. Hence the initial nodal temperature of the domain was assumed to be the value sufficient enough to start the simulation. It was provided to be $1500K$ which is in between the ignition temperature of iron and melting temperature of iron oxide and hence sufficient enough to start the simulation. The convective heat transfer condition was confined within each boundary of the solution domain, and the coefficient of the convective heat transfer was set to $155W/m^2K$. The heat loss associated with the leakage of the melted material was taken into account. The heat flow through the model was then simulated using numerical method (CM), and the simulation started when the heat source approached the solution domain and lasted until the all the cells of the solution domain are melted thereby forming the cut. The steady state solution is sought assuming proper boundary conditions and heat input.

The dimensions of the steel being modelled was: 300 mm in length (x direction). The mesh consisted of 121 nodes. V was the speed of the torch which was set to $400mm/min$. The heat input generated by the different exothermic chemical reactions taking place in the flame during cutting was assumed to be uniformly distributed. The physical properties of the steel being used were as shown in the table 6-1.

Thermal Conductivity	43.0 W/(m-K)
Density	7750 kg/m^3
specific heat capacity	490 J/(kg-K)
latent heat of melting	209*1000 J/kg
latent heat of melting	1810 K

Table 6-1: The physical properties of steel being used.

The results obtained with a numerical simulation were compared to those obtained in the experiment in the section 5-3-2 in order to verify the model used in the heat flow simulation with the models proposed for the heat sources. The temperature profile plot obtained by the simulation of the model is shown in figure 6-2. And the temperature profile plot obtained by performing the experiments is shown in 5-5. We can establish the fact that the two results matched relatively well for the numerical model to be feasible for use in further analyses of the cutting process. However since the simulation was performed only once the cut starts hence the heat associated with the preheating phase is not captured in the plot. Also the simulation results shows just the line of cut and not the surrounding material hence the temperature distribution is depicted only for the cut zone whereas in 5-5 the plot shows the temperature distribution to the enclosed material as well.

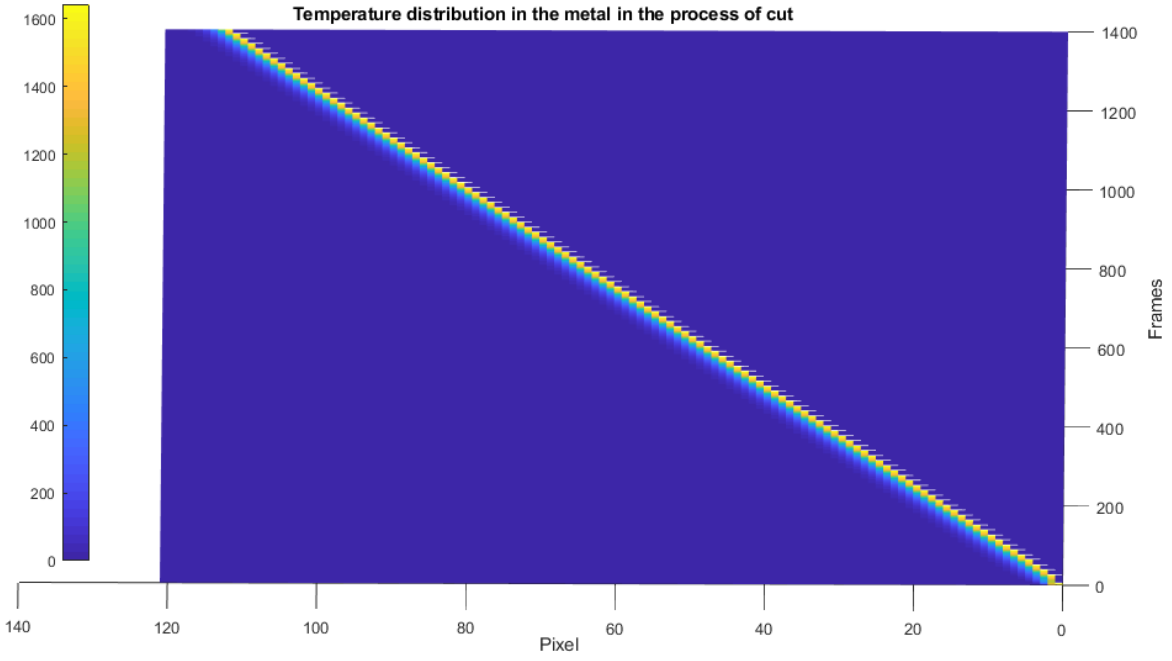

Figure 6-2: Temperature profile obtained from the simulation

Chapter 7

Conclusion

The model for heat flow and phase change during melting process were proposed for oxy-acetylene flame cutting of steel plates in order to determine the feasibility of an automatic cutting process control. Numerical simulations based on the Cell Method were carried out for the proposed models to analyze the heat flow through the work piece during cutting. A series of experiments were also performed in order to produce a range of cuts and to verify the results of the simulation and to evaluate the proposed models for the heat sources with respect to variations in the cutting parameters.

A comparison was made between the results predicted through the simulation and obtained through the experiment, and the following conclusions were made:

- The proposed model of heat flow in the cutting process and the corresponding temperature distribution are adequate for use to analyze heat flow on a work-piece, showing that temperature histories on the work-piece during cutting were in fair agreement with those obtained through the experiment.
- Since the identification of the parameters were not done and few of the parameters in the simulation is chosen arbitrarily, hence the discrepancy in the result is expected.
- The experimental data has shown that the material thickness do not affect the temperature control parameters in any significant way.

Chapter 8

Future Work

The following future work is recommended in order to be able to successfully automate the cutting process:

- The identification of the parameters for the obtained model could be done to be able to perfectly match the simulated model with the experimental results.
- The feasibility study to evaluate the oxyfuel gas cutting process, through experimental data and literature search, has shown that flame-cut quality depends upon the temperature of the metal at the cut and the proper combustion mixture of oxygen and metal. These two conditions are interactive because both the torch travel speed and the cutting oxygen affect the metal temperature and the oxygen-metal mixture. The preheat flame, however, primarily affects the metal temperature and provides kindling temperature for cut initiation. Since the speed, cutting oxygen, and preheat interact and have overlapping effects, hence in order to be able to automate the cutting process it is necessary to identify variables which could be used to sort out the cutting parameters and determine which should be adjusted when cut quality began to deteriorate. Hence the modelling of heat source and the chemical reactions could be further done.
- The model obtained is 1D transient heat conduction and phase change during cutting. This can be modified to be able to create a 3-D model in order to be able to realize in the practical scenario.

Bibliography

[1] E. Tonti, *The Mathematical Structure of Classical and Relativistic Physics*. Birkhäuser Basel, 2013.

[2] TWI, "Oxyfuel cutting - process and fuel gases."

[3] J. Powell, D. Petring, R. V. Kumar, S. O. Al-Mashikhi, A. F. H. Kaplan, and K. T. Voisey, "LaserâĂŞoxygen cutting of mild steel: the thermodynamics of the oxidation reaction," *Journal of Physics D: Applied Physics*, vol. 42, no. 1, p. 015504, 2009.

[4] S. Sheng, Paul, and V. S. Joshi, "Analysis of heat-affected zone formation for laser cutting of stainless steel," vol. 53, p. 879âĂŞ892, 09 1995.

[5] A. Adedayo, "Kinetics of oxyfuel gas cutting of steels.," vol. 33, pp. 183–188, 2011.

[6] P. P. Vilaca, "Oxyfuel gas welding and cutting, department of engineering. design and production," February 2015.

[7] G. V. Slottman and E. H. Roper, *Oxygen cutting*. 1951.

[8] K. J. B. G. Ivarson A, Powell J and M. C, "The effects of oxygen purity in laser cutting mild steel.," vol. 299, p. 95âĂŞ101, 1993.

[9] K. T. M. M. Terasaki, T., "Heat input generated in plate by gas cutting process.," vol. 10, p. 197âĂŞ204, 2009.

[10] S. J. I. M. O. M. Osawa, N., "Study of heat transfer during piercing process of oxyfuel gas cutting.," vol. 56, pp. 2–10, 2012.

[11] M. S. Y. Bae K Y, Yang Y S, "Numerical analysis of heat flow in oxy-ethylene flame cutting of steel plate," 2016.

[12] E. Tonti, "Why starting from differential equations for computational physics?," *Journal of Computational Physics*, pp. 1260–1290, 2013.

[13] E. Ferretti, "The mathematical foundations of the cell method," pp. 362–379, 2015.

[14] E. Ferretti, "The algebraic formulation: Why and how to use it," p. 106âĂŞ149, 2015.

[15] E. Ferretti, "The cell method: An overview on the main features," p. 194âĂŞ243, 2015.

[16] K. O. Z. A. Ermolaev, G., "Parameterization of hybrid laser assisted oxygen cutting of thick steel plates.," vol. 47, p. 95âĂŞ101, 2013.

[17] G. J. O'Neill, W., "New developments in laser-assisted oxygen cutting.," vol. 34, p. 355âĂŞ367, 2000.

[18] N. OSAWA, J. SAWAMURA, Y. IKEGAMI, and K. YAMAGUCHI, "Study on the relationship between the heat transfer characteristics of preheating gas and cutting performance of oxyfuel gas cutting," *QUARTERLY JOURNAL OF THE JAPAN WELDING SOCIETY*, vol. 31, no. 2, pp. 141–156, 2013.

[19] HGG, "Oxy fuel cutting: The basics explained."

[20] K. Mori, "Kinetics of fundamental reactions pertinent to steelmaking process," vol. 28, pp. 246–261, 1988.

[21] K. Mondal, H. Lorethova, E. Hippo, T. Wiltowski, and S. B. Lalvani, "Reduction of iron oxide in carbon monoxide atmosphere - reaction controlled kinetics," *Fuel Processing Technology - FUEL PROCESS TECHNOL*, vol. 86, pp. 33–47, 11 2004.

[22] P. M. D. M. D. R. Muñoz-Escalona, P., "Analysis and influence of acetylene and propane gas during oxyfuel gas cutting of 1045 carbon steel.," vol. 15, p. 684âĂŞ692, 2006.

[23] M. A. R. Dogan N, Geoffrey A. Brooks, "Kinetics of decarburization reaction in oxygen steelmaking process," pp. 9–11, 2010.

[24] J. W. Giachino, *Oxy-Acetylene Welding and Cutting*. 1942.

[25] H. B. Callen, *Thermodynamics*. JOHN WILEY & SONS, INC., 1960.

[26] D. Rosenthal, "Mathematical theory of heat distribution during welding and cutting.," vol. 20, pp. 220–234, 1941.

[27] L. Lindgren, "Finite element modeling and simulation of welding. part 1: increased complexity.," vol. 24, p. 141âĂŞ192, 2001.

[28] G. P. Nikishkov, "Introduction to the finite element method," 2004.

[29] A. Mohammed Sifullah, N. Yusoff, M. Hassan, and A. Hossain, "Finite element analysis of fusion laser cutting on stainless steel-304," vol. 11, pp. 181–189, 01 2016.

[30] R. M. Ferrari, F. Boem, and T. Parisini, "An algebraic approach to modeling distributed multiphysics problems: the case of a dri reactor," *IFAC-PapersOnLine*, vol. 48, no. 17, pp. 155 – 160, 2015.

[31] E. Tonti, "A direct discrete formulation of field laws: the cell method," vol. 1, p. 11, 01 2001.

[32] M. C. E. Manuel, S.-P. Lin, W.-H. Lu, and P. T. Lin, "Errors in thermographic camera measurement caused by known heat sources and depth based correction," *International Journal of Automation and Smart Technology*, vol. 6, no. 1, 2016.

[33] "Optotherm thermal imaging, url = https://www.optotherm.com/emiss-calculating.htm,."

[34] K. E. B.V., "Koike cutting nozzles," 2016.

[35] T. Blomberg, "Heat conduction in two and three dimensions : computer modelling of building physics applications," vol. 1008, p. 188, 1996.

[36] M. R. Piergiorgio Alotto, Fabio Freschi and C. Rosso, "The cell method for electrical engineering and multiphysics problem," 2013.